MOLECULAR AND CELLULAR BIOLOGY, Apr. 2010, p. 1958–1970 Vol. 30, No. 8
0270-7306/10/$12.00 doi:10.1128/MCB.01437-09

The Nematode Eukaryotic Translation Initiation Factor 4E/G Complex Works with a *trans*-Spliced Leader Stem-Loop To Enable Efficient Translation of Trimethylguanosine-Capped RNAs▽†

Adam Wallace,[1] Megan E. Filbin,[1,2] Bethany Veo,[1] Craig McFarland,[1] Janusz Stepinski,[3] Marzena Jankowska-Anyszka,[4] Edward Darzynkiewicz,[3] and Richard E. Davis[1,2]*

Department of Biochemistry and Molecular Genetics[1] and Molecular Biology Program,[2] University of Colorado School of Medicine, Aurora, Colorado 80045; Division of Biophysics, Institute of Experimental Physics, Faculty of Physics, University of Warsaw, 02-089 Warsaw, Poland[3]; and Faculty of Chemistry, University of Warsaw, 02-093 Warsaw, Poland[4]

Received 31 October 2009/Returned for modification 14 December 2009/Accepted 2 February 2010

Eukaryotic mRNA translation begins with recruitment of the 40S ribosome complex to the mRNA 5′ end through the eIF4F initiation complex binding to the 5′ m^7G-mRNA cap. Spliced leader (SL) RNA *trans* splicing adds a trimethylguanosine (TMG) cap and a sequence, the SL, to the 5′ end of mRNAs. Efficient translation of TMG-capped mRNAs in nematodes requires the SL sequence. Here we define a core set of nucleotides and a stem-loop within the 22-nucleotide nematode SL that stimulate translation of mRNAs with a TMG cap. The structure and core nucleotides are conserved in other nematode SLs and correspond to regions of SL1 required for early *Caenorhabditis elegans* development. These SL elements do not facilitate translation of m^7G-capped RNAs in nematodes or TMG-capped mRNAs in mammalian or plant translation systems. Similar stem-loop structures in phylogenetically diverse SLs are predicted. We show that the nematode eukaryotic translation initiation factor 4E/G (eIF4E/G) complex enables efficient translation of the TMG-SL RNAs in diverse *in vitro* translation systems. TMG-capped mRNA translation is determined by eIF4E/G interaction with the cap and the SL RNA, although the SL does not increase the affinity of eIF4E/G for capped RNA. These results suggest that the mRNA 5′ untranslated region (UTR) can play a positive and novel role in translation initiation through interaction with the eIF4E/G complex in nematodes and raise the issue of whether eIF4E/G-RNA interactions play a role in the translation of other eukaryotic mRNAs.

Cap-dependent translation initiation in eukaryotes is a complex process involving many factors and serves as the primary mechanism for eukaryotic translation (37, 44). The first step in the initiation process, recruitment of the m^7G (7-methylguanosine)-capped mRNA to the ribosome, is widely considered the rate-limiting step. It begins with recognition of and binding to the m^7G cap at the 5′ end of the mRNA by the eukaryotic translation initiation factor 4F (eIF4F) complex, which contains three proteins: eIF4E (a cap-binding protein), eIF4G (a scaffold protein with RNA binding sites), and eIF4A (an RNA helicase). eIF4G's interaction with eIF3, itself a multisubunit complex that interacts with the 40S ribosome, facilitates the actual recruitment of capped RNA to the ribosome. With the help of several other initiation factors, the small ribosomal subunit scans the mRNA from 5′ to 3′ until a translation initiation codon (AUG) in appropriate context is identified and an 80S ribosomal complex is formed, after which the first peptide bond is formed, thus ending the initiation process (37, 44). The AUG context can play an important role in the efficiency of translation initiation (23, 44). The length, structure, and presence of AUGs or open reading frames in the mRNA 5′ untranslated region (UTR) can negatively affect cap-dependent translation and ribosomal scanning. In general, long and highly structured 5′ UTRs, as well as upstream AUGs leading to short open reading frames, can impede ribosome scanning and lead to reduced translation (23, 44). In addition, 5′ UTRs less than 10 nucleotides (nt) in length are thought to be too short to enable preinitiation complex assembly and scanning (24). Thus, several attributes of the mRNA 5′ UTR are known to negatively affect translation initiation, whereas only the AUG context and the absence of negative elements are known to have a positive effect on translation initiation (44).

Two of the important mRNA features associated with cap-dependent translation, the cap and the 5′ UTR, are significantly altered by an RNA processing event known as spliced leader (SL) *trans* splicing (3, 8, 17, 26, 36, 47). This takes place in members of a diverse group of eukaryotic organisms, including some protozoa, sponges, cnidarians, chaetognaths, flatworms, nematodes, rotifers, crustaceans, and tunicates (17, 28, 39, 55, 56). In SL *trans* splicing, a separately transcribed small exon (16 to 51 nucleotides [nt]) with its own cap gets added to the 5′ end of pre-mRNAs. This produces mature mRNAs with a unique cap and a conserved sequence in the 5′ UTR. In metazoa, the m^7G cap is replaced with a trimethylguanosine (TMG) cap ($m^{2,2,7}$GpppN) (27, 30, 46, 49). In nematodes, ~70% of all mRNAs are *trans* spliced and therefore have a TMG cap and an SL (2). In general, eukaryotic eIF4E proteins do not effectively recognize the TMG cap (35). This raises the issues of how the translation machinery in *trans*-splicing

* Corresponding author. Mailing address: Department of Biochemistry and Molecular Genetics, University of Colorado School of Medicine, Mailstop 8101, Bldg. RC-1S, Rm. 10401G, 12801 E. 17th Ave., Aurora, CO 80045. Phone: (303) 724-3226. Fax: (303) 724-3215. E-mail: Richard.davis@ucdenver.edu.

† Supplemental material for this article may be found at http://mcb.asm.org/.

▽ Published ahead of print on 12 February 2010.

metazoa effectively recognizes TMG-capped *trans*-spliced mRNAs, what role the SL sequence plays in translation initiation, and how the conserved translation initiation machinery has adapted to effectively translate *trans*-spliced mRNAs.

Previous work has shown that efficient translation of TMG-capped messages in nematodes requires the SL sequence (22 nt) immediately downstream of the cap (5, 25, 29). In the current studies, we sought to understand the manner in which the SL enhanced the translation of TMG-capped mRNAs. Using a cell-free nematode *in vitro* translation system, we carried out mutational analyses that define the specific sequences in the SL that are required and sufficient for efficient translation of TMG-capped mRNAs. These analyses led to the discovery of a small, discrete stem-loop immediately adjacent to the TMG cap in *trans*-spliced messages required for efficient translation. Notably, the sequences involved in the base pairing of the stem are highly conserved in alternative SL sequences found in nematodes. We further show that the nematode eIF4E/G complex plays a major role in facilitating the SL enhancement of TMG-capped mRNA that likely occurs after the initial cap-binding step. The results demonstrate the importance of specific enhancing elements in the 5′ UTR and adaptation in the eIF4F complex necessary for optimal cap-dependent translation.

MATERIALS AND METHODS

Cell-free translation. Whole-cell extracts were prepared from *Ascaris* embryos as previously described, except in some cases in which they were not dialyzed (25). Translation assays were carried out without nuclease treatment of the extracts under competitive translation conditions that mimicked translation *in vivo* (5, 25). Translation was carried out with the addition of reporter luciferase RNAs to the reaction mixture at 1 to 2.5 μg/ml, and translation was conducted for 40 to 60 min at 30°C. Luciferase assays were carried out as described previously (5, 25).

Extracts were depleted of the eIF4F complex essentially as described previously (10, 11). In brief, 200 μl of *Ascaris* embryo extract was incubated with 250 μl of m^7GTP-Sepharose 4B beads (GE Healthcare, Piscataway, NJ) equilibrated in translation dialysis buffer (20 mM Tris-HCl [pH 7.8], 50 mM KCl, 0.2 mM EDTA, 1 mM dithiothreitol [DTT], and 20% glycerol) at 4°C for 15 min with slow rotation. The samples were centrifuged at 800 × *g* for 2 min at 4°C, and the supernatant (depleted extract) was collected and immediately frozen. To reconstitute the depleted extract with recombinant proteins, either *Ascaris* eIF4G-4E3 complex at ~12.5 ng/μl or wheat germ eIF4F, -4A, and -4B complex at 175 ng/μl was mixed with an equal volume of depleted extract so that a 10-μl reconstituted reaction mixture contained 25 ng luciferase mRNA, ~3 ng of *Ascaris* protein, or 43.75 ng of wheat germ protein or an equivalent volume of buffer, 2.5 μl of depleted extract, and 1× translation buffer (25). As a control for 4G and 4E activity, 4E binding peptide (4E-BP) (RIIYDRKFLMECRNSPV) was added to reconstitution reaction mixtures at a final concentration of 45.4 μM. In those cases, the protein was preincubated with peptide at 30°C for 10 min. Translation assays were then carried out as previously described (25).

Wheat germ translation assays supplemented with recombinant proteins were carried out in a manner similar to that described for *Ascaris* translation assays. Briefly, a 20-μl reaction mixture contained 125 mM KOAc, 2.6 mM MgOAc, 0.5 mM GTP, 0.5 mM ATP, 10 mM creatine phosphate, 50 μg/ml creatine kinase, 2 mM DTT, and 50 μM amino acid mix with 0.625 ng/μl of luciferase RNA, either 62.5 ng/μl of recombinant *Ascaris* eIF4G-4E3 or 42 ng/μl of recombinant wheat germ 4G-4E or the equivalent volume of buffer, and 2.5 μl of prepared wheat germ extract. Prior to addition of the extract, all other components were preincubated at 30°C for 5 min and returned to ice. Upon addition of the extract, reactions were incubated at 25°C for 2 h. Each reaction mixture was diluted at 1:25 into cold 1× passive lysis preparation, and luciferase activity measurements were obtained as previously described (18).

eIF4E-3 and eIF4G expression. *Ascaris* eIF4E-3, which is the dominant isoform of eIF4E in early embryos and recognizes both monomethyl- and trimethylguanosine caps, has previously been described (25). Fragments of *Ascaris* eIF4G were generated using degenerate PCR and then 5′ and 3′ rapid amplification of cDNA ends (RACE) (GenBank accession no. GQ373389). By the use of the sequence from these portions of the eIF4G mRNA, the full-length *Ascaris* eIF4G open reading frame (see Fig. S1 in the supplemental material) was amplified by PCR (using GACGACGACAAGATCAGGTTCAAACTTACTA TGTCCAGTAG and CGCGGGCGGCCGTTCTTAATTGAGCAACTCATA GAGATTTTC primers). Purified PCR products were treated with T4 DNA polymerase and simultaneously annealed into pET30a with an LIC Duet miniadaptor (Novagen, Madison, WI) to form a plasmid that would coexpress both proteins. The final construct, as confirmed by sequencing, consisted of eIF4G in the orf1 position with an N-terminal 6× His tag followed by the miniadaptor and then eIF4E-3 in the orf2 position. The plasmid, called 4G-Mini-4E3-pET30, was transformed into the Rosetta 2 DE3 expression strain (Novagen). A 1-liter volume of culture at an optical density at 600 nm (OD_{600}) of 0.4 in LB-kanomycin (30 μg/ml) was induced by adding IPTG (isopropyl-β-D-thiogalactopyranoside) to achieve a final concentration of 0.2 mM and was incubated with shaking at 16°C for 24 h. Cells were harvested and stored at −80°C. The cell pellet was resuspended in 20 ml of lysis buffer (20 mM HEPES-KOH [pH 7.5], 300 mM urea, 200 mM NaCl, 100 mM KCl, 10% glycerol, 10 mM imidazole, 1 mM DTT, 2 Complete Mini EDTA-free protease inhibitor tablets [Roche, Indianapolis, IN], and 1 μg/ml lysozyme) and incubated on ice for 30 min. The lysate was then sonicated on ice for 10 min at power setting 7.5 using 10-s pulses with 20-s rests (Misonix Sonicator 3000; Fisher Scientific). The sonicated sample was clarified by centrifugation at 16,000 × *g* for 20 min at 4°C. The resulting supernatant was incubated with 1 ml nickel-nitrilotriacetic acid (Ni-NTA) beads (Qiagen) that had been equilibrated with His wash buffer (20 mM HEPES-KOH [pH 7.5], 300 mM urea, 200 mM NaCl, 100 mM KCl, and 10% glycerol) for 1 h at 4°C on a nutator. Protein was eluted from the Ni-NTA beads by using a stepwise gradient of imidazole concentrations in His wash buffer. Eluates (1 ml) were analyzed using sodium dodecyl sulfate-polyacrylamide gel electrophoresis (SDS-PAGE), and the three eluates containing the eIF4E/G complex were collected. The sample buffer was exchanged using buffer-20 (20 mM HEPES-KOH [pH 7.6], 20 mM KCl, 0.1 mM EDTA, 1 mM DTT, and 10% glycerol) and an Amicon Ultra-4 centrifugal filter device (Millipore) (100-K cutoff). SDS-PAGE analysis revealed the two protein bands of interest (eIF4G at ~170 kDa and eIF4E-3 at ~26 kDa), constituting ~40% of the total protein in the sample.

RNA preparation. Reporter RNAs (Renilla or Gaussia luciferase with an 85-nt adenylate tail) were transcribed from PCR templates by the use of T7 RNA polymerase and an Ambion Megascript kit and purified as previously described (5, 25). Cap priming was carried out at a ratio of 8:1 for cap:GTP by the use of m^7GpppG or $m^{2,2,7}$GpppG prepared as described previously (5, 25). Transcription reaction mixtures were treated with DNase I and extracted with TRIzol (Invitrogen, Carlsbad, CA), and the RNAs were precipitated twice, once with isopropanol and then with ammonium acetate-ethanol. Precipitated RNAs were further washed with 70% ethanol, dissolved in water, quantitated spectrophotometrically, and examined by agarose-formaldehyde denaturing gel electrophoresis. The 5′ UTR sequences used are illustrated in the figures for each experiment (shown as DNA sequences), and the 3′ UTRs were as previously described (5, 25).

SL mutations. Blocks of random mutations in the RNAs were introduced using primers that incorporated N into PCR templates at specific positions, resulting in transcribed RNAs with all four nucleotides represented at the N position. Specific nucleotide substitutions were prepared using PCR primers to generate mutant PCR templates, with the corresponding mutant RNAs transcribed *in vitro* as described above.

RNA stability and 5′ monophosphate RNA analysis. ^{32}P-labeled transcripts were synthesized using Promega's Riboprobe *in vitro* transcription system (Madison, WI) as described previously (5, 25). For stability analyses, uniformly labeled RNAs were added to the cell-free translation system, purified at different time points, and electrophoretically separated under denaturing conditions, and the amount of RNA remaining was determined by phosphorimager analysis using a Molecular Dynamics STORM 860 phosphorimager and ImageQuant software. Monophosphate RNAs (5′) were produced using RNA priming with a GMP:GTP ratio of 40:1. Dcp2 decapping of an mRNA in the extract would generate an RNA with a 5′ monophosphate (pGN_x... versus $TMGpppGN_x$.....). Monophosphate RNA (5′) was used to mimic decapped RNA in stability assays. For analysis of the amount of 5′ monosphosphate RNAs produced during translation in the cell-free system, RNAs were isolated at various time points and treated with Terminator 5′ phosphate-dependent exonuclease (Epicentre, Madison, WI) and the RNAs were analyzed and quantified by phosphorimager analysis of denaturing gel electrophoresis separations. Terminator is a 5′ → 3′ exonuclease

(Epicentre) that is highly specific for RNAs with a 5′ monophosphate and does not degrade capped, 5′ triphosphate, or diphosphate RNA (52).

SPR. The binding of proteins to short RNAs was analyzed using a BIACORE 3000 surface plasmon resonance (SPR) instrument (Biacore, Uppsala, Sweden) and Sensor Chip SA (GE Healthcare Bio-Sciences AB, Uppsala, Sweden). The chip was conditioned by three injections of 100 μl of 1 M NaCl–50 mM NaOH at a flow rate of 100 μl/minute. HBS-P buffer (GE Healthcare Bio-Sciences AB) (0.01 M HEPES [pH 7.4], 0.15 M NaCl, 0.005% Surfactant P-20) was used as a running buffer at a flow rate of 20 μl/min. Immobilization of ligand RNA was a two-step process. First, 40 μl of 2 μM biotinylated oligo$(dT)_{23}$ was immobilized on all four channels (saturated response). Then, 30 μl of 2 μM RNA [consisting of 41-nt RNA with 20 additional As for a 3′ poly(A) tail] was bound to each channel through dT/A base pairing. The responses for each RNA immobilization were observed to be relatively similar for all channels (1,700 to 1,900 relative units). A 100-μl volume of purified recombinant *Ascaris* 4E-3/4G complex at various concentrations (1.73 nM, 3.45 nM, 6.9 nM, 13.8 nM, and 27.6 nM) was injected on all four channels, and response was measured. The chip was regenerated using 40 μl of 6 M guanidine-HCl (pH 2.2). The data were analyzed using Scrubber-2 software (University of Utah, Salt Lake City, UT), and the bulk refractive index was floated to fit the data.

Sucrose gradient analysis of translation reactions. Translation reactions were analyzed on sucrose gradients prepared in polypropylene tubes (Seton Scientific, Los Gatos, CA) (14 by 89 mm) by layering equal volumes of 5% sucrose on 25% sucrose (5% or 25% sucrose, 50 mM Tris-HCl [pH 7.5], 50 mM NaCl, 5 mM $MgCl_2$, 1 mM DTT, 100 μg/ml cycloheximide). Gradients were formed using a Gradient Station apparatus (Biocomp, Fredericton, New Brunswick, Canada). Cell-free translation reactions were performed using micrococcal nuclease-treated *Ascaris* extract scaled up to 200 μl and preincubated with 0.5 mM cycloheximide for 5 min at 30°C. Translation reactions were initiated by the addition of 250 ng of universally ^{32}P-labeled RNA. Following an incubation of 30 min at 30°C, reaction mixtures were diluted with an equal volume of cold homogenization buffer (100 mM Tris-HCl [pH 7.5], 100 mM NaCl, 40 mM $MgCl_2$, 300 μg/ml cycloheximide, 100 μg/ml heparin) and 40 μl of 10× detergent solution (5% Trition X-100, 121 mM sodium deoxycholate). Samples were layered on top of the gradients and centrifuged at 36,000 rpm for 3 h at 4°C in a SW41 Ti rotor (Beckman Coulter, Inc., Fullerton, CA). Sucrose gradients were fractionated using a Gradient Station apparatus (Biocomp) and an FC203B fraction collector (Gilson, Inc., Middleton, WI). Fractions (350 μl) were collected, and radioactivity was detected using Cerenkov counting. During fractionation, the absorbance at 254 nm was recorded using a Pharmacia Biotech UV-MII lamp (1-*A* sensitivity) and RecIII recorder (GE Healthcare, Piscataway, NJ) (0.2 V, 20 mm/min).

RESULTS

SL sequence and translation of TMG-capped RNAs. To examine the function of the SL sequence in translation, we used a nematode embryo cell-free translation system that is cap and poly(A)-tail dependent, exhibits cap-tail synergism, and reproduces characteristics of *trans*-spliced mRNA translation observed *in vivo*, including the ability of the SL sequence to stimulate translation of TMG-capped RNAs (5, 25). As previously observed, TMG-capped RNA translation is less efficient than m^7G-capped RNA translation in the nematode cell-free system (see Fig. 1A; compare columns 1 and 2). Replacement of the first 22 nt of the test RNA with the nematode SL1 sequence significantly enhanced translation of the TMG-capped RNA but did not significantly stimulate translation of m^7G-capped RNA (Fig. 1A; compare columns 1 and 3 to columns 2 and 4). Efficient translation of the TMG-capped RNA appears to be dependent on sequences within the spliced leader, since substitution of random sequences for the SL did not facilitate translation of the TMG-capped RNA (Fig. 1A; compare columns 5 and 6). Overall, these data show that the SL is needed for efficient translation of TMG-capped mRNAs.

Key regions of the SL required for TMG cap translation. To determine the specific sequences within the spliced leader that contribute to translation of TMG-capped mRNAs, we tested a series of random 4-nt substitutions across the entire SL in the *in vitro* translation system (Fig. 1B). Mutations in two regions of the SL, Mut-1 and Mut-3, led to significant reductions in the translation of the TMG-capped luciferase reporter (Fig. 1B). Similar results were obtained using a second luciferase reporter RNA (Gaussia luciferase) with the SL sequence placed immediately upstream of the reporter AUG (Fig. 1C). The configuration of the SL relative to the AUG in these two 5′ UTRs corresponds to the two major types of native *trans*-spliced 5′ UTRs on nematode mRNAs (25). We next determined whether the SL mutations in blocks 1 and 3 were additive by evaluating translation of a double mutant, Mut-7. The reduction in translation observed in Mut-7 was only slightly greater than that seen with either Mut-1 or Mut-3 (Fig. 1B). To determine whether the Mut-1 and Mut-3 mutations reduced luciferase expression by decreasing mRNA stability, we examined the decay of the reporter RNAs during translation. Mut-1 and Mut-3 RNAs were slightly more stable than RNA with the wild-type (WT) SL during translation (Fig. 1D). Similar results were obtained for the second Gaussia luciferase reporter RNA (data not shown). Therefore, mutations in the SL inhibit translation and not RNA stability.

To test the possibility that mutations in blocks 1 or 3 led to decapping of mutant versus wild-type SL RNA, we examined the rate of decay of 5′ monophosphate RNAs (the products of RNA decapping) and compared the amounts of decapped RNAs derived from wild-type or mutant SL mRNAs that accumulated during translation in the extracts. These analyses demonstrated that decapping of mRNAs with the wild-type SL was not different from decapping of mRNAs with the mutant SLs (see Fig. S2 in the supplemental material). We conclude from these data that SL nucleotides within blocks 1 and 3 promote translation of capped mRNAs.

Specific SL nucleotides are necessary and sufficient for translation of TMG-capped RNAs. To determine the contribution of individual nucleotides within blocks 1 and 3, we examined random 2-nt mutations. All 2-nt sets within these regions contribute to the translation of TMG-capped mRNAs (see Fig. S3A and B in the supplemental material). We used blocks of random nucleotides in a nonbiased and rapid approach to define sequences that contribute to this translation effect. However, as each 4-nt block of substitutions represents 256 different RNA transcripts, we predicted that the observed reductions in translation are likely underestimates of the total effect of altering these nucleotides. We next examined several specific nucleotide mutations in block 3 for their effect on translation. Specific nucleotide substitutions led to a significant reduction in translation (Fig. 2A; GGGT-Mut-3 levels were only 3% of wild-type levels). Single nucleotide substitutions in block 3 and SL nt 14 (not previously tested as part of a Renilla block mutation) also greatly reduced translation (Fig. 2B). Finally, substitution of the first nucleotide of the SL (G → A) or deletion of this G led to a reduction in translation (Fig. 2B). Thus, specific nucleotides within the SL are required for translation of TMG-capped RNA in nematodes.

We next determined which SL sequences were sufficient for optimal translation of a TMG-capped RNA by comparing the translation of RNAs with fixed regions of SL sequence combined with other randomized regions (Fig. 2C). Although mu-

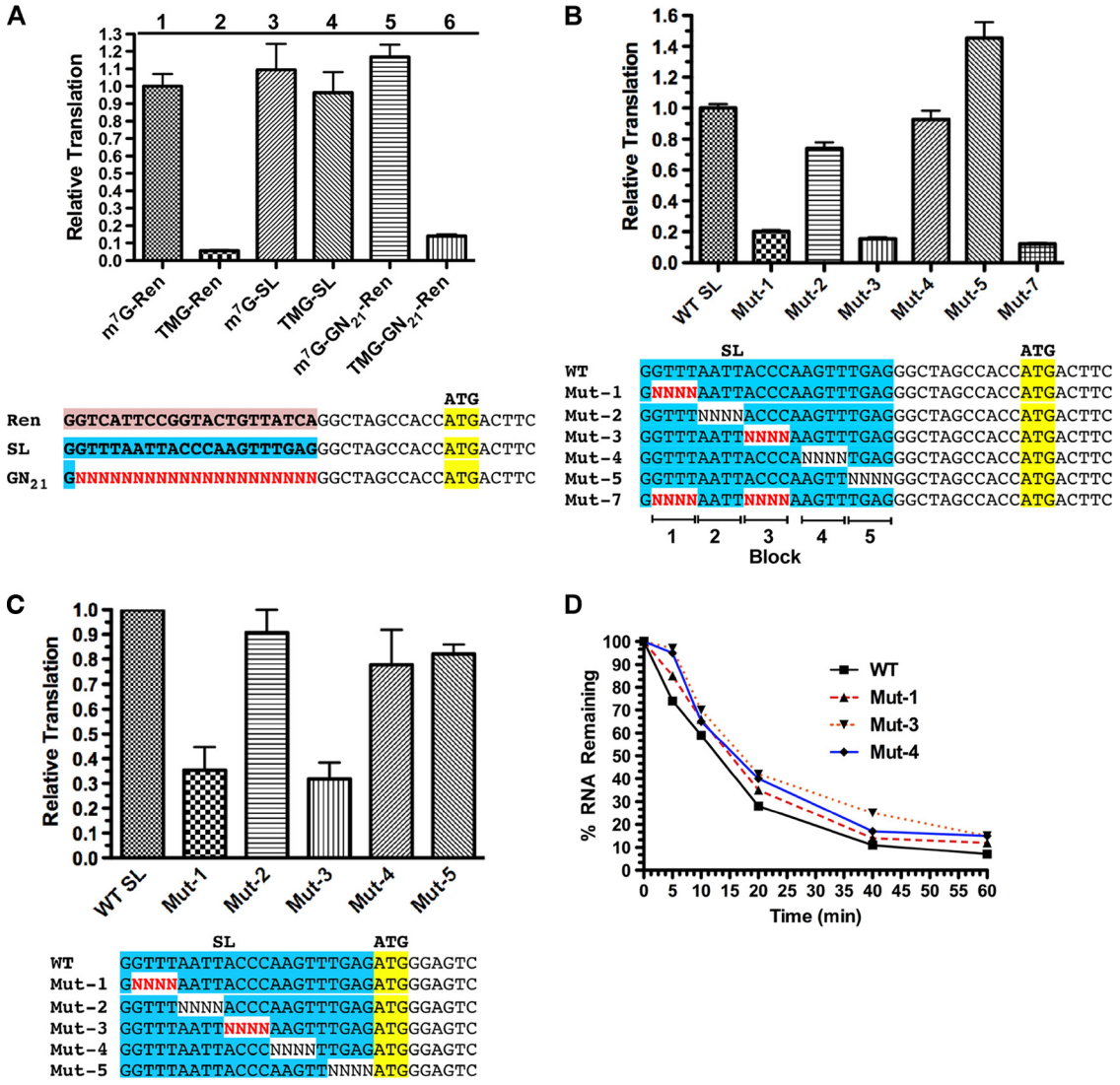

FIG. 1. Two regions within the SL are required for optimal translation of TMG-capped RNAs. (A) The spliced leader sequence is required for efficient translation of TMG-capped RNAs. Renilla luciferase reporter RNAs with a 3′ 85-nt polyadenylate tail were transcribed *in vitro* and translated in an *Ascaris* embryo cell-free translation system. RNA differences included the type of cap (m^7G, m^7GpppG; TMG, $m^{2,2,7}GpppG$) and sequences in the 5′ UTR as illustrated. Translation levels were set at 1 for the m^7GpppG-capped RNA with the Renilla 5′ UTR (m^7G-Ren). Translation of this m^7G-capped Renilla RNA resulted in $\sim 1.5 \times 10^7$ relative light units (RLUs)/ng of RNA in the extracts. (B) Random block mutations within the SL define two regions that contribute to translation of TMG-capped Renilla luciferase RNA. N, all four nucleotides represented at these positions in the DNA template and translated RNA. (C) Translation of Gaussia luciferase RNA with the SL and its mutants immediately adjacent to the AUG codon defines the same two regions within the SL important for translation of TMG-capped RNA. (D) Stability of RNAs with block mutations in the SL is not decreased during translation in the extracts. The percentages of 1,100-nt Renilla RNA remaining were calculated as a function of time and plotted. Note that RNAs with mutations in the SL and decreased translation (Mut-1 and Mut-3) did not exhibit reduced RNA stability during the translation period.

tations in blocks 1 and 3 of the SL led to the most dramatic reductions in translation, these two regions alone were not able to fully rescue translation of TMG-capped RNA. However, blocks 1, 3, and 4 that included the native nucleotide 14 were able to translate TMG-capped RNA as efficiently as the wild-type SL sequence. The key block 4 residue was the A at nucleotide 14 (Fig. 2D and data not shown). Thus, the core SL sequence sufficient for optimal translation when the TMG cap is present is GGUUUNNNNACCCANNNNNNNN.

Core SL sequences contribute to the RNA secondary structure required for translation of TMG-capped RNA. Examination of the SL sequence led to the identification of a potential stem-loop structure in the 5′ end of the SL (Fig. 3A). To determine whether the stem contributed to facilitating translation of TMG-capped RNAs, we tested RNAs in which each side of the stem was altered to disrupt potential base pairing along with a double mutant that restored the stem base pairing (Fig. 3B). The mutations that disrupted the putative stem led to significant reductions in translation, but when the two mutations were combined to restore base pairing, translation was also restored (Fig. 3D). As is consistent with these observations, selective 2′-hydroxyl acylation analyzed by primer exten-

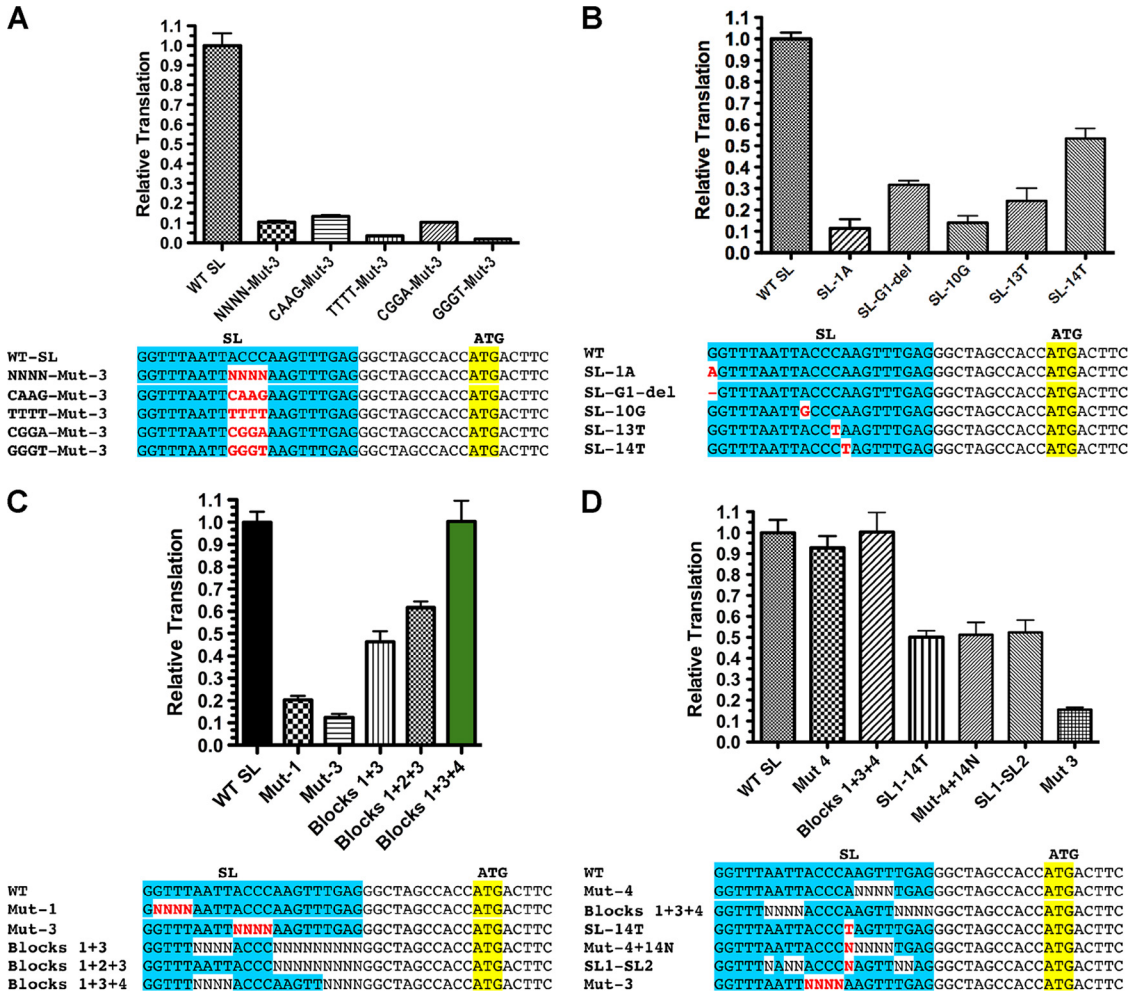

FIG. 2. Sequences necessary and sufficient for optimal translation of TMG-capped RNAs. (A) Fixed nucleotide substitutions within block 3 further reduced translation of TMG-capped RNAs. For the comparisons, WT SL translation was set to 1. (B) Single nucleotide substitutions significantly reduce translation of TMG-capped RNAs. (C) Sequences within blocks 1, 3, and 4 are necessary and sufficient for optimal translation of TMG-capped RNAs. (D) Nucleotide 14 is the key residue in block 4 required for optimal translation of TMG-capped RNAs. Experiments were carried out as described for Fig. 1.

sion (SHAPE) (33, 51) demonstrated that some of the core SL sequences were constrained and that mutations in block 3 (ACCC → GGGU) led to increased flexibility in blocks 1 and 3 (see Fig. S4 in the supplemental material). Together, these data demonstrate that a small stem-loop at the 5′ end of the SL plays an important role in translation of TMG-capped RNAs.

The position and spacing of the SL determine its activity. We next examined whether spacing between the stem and block 1 nucleotides is important. Separation of the TMG cap and block 1 by as little as 2 random nucleotides dramatically reduced translation (Fig. 3E). We next examined the importance of spacing between the two key blocks of residues (blocks 1 and 3) by evaluating the effect of increasing the distance between these elements. Spacing of more than 2 nt significantly reduced the overall translation (Fig. 3F). We conclude that spacing between the TMG cap, block 1, and block 3 is important to translation, which in turn suggests that the loop, its length, and its location with respect to the cap are important for translation.

The nematode eIF4E/G complex, but not the wheat germ eIF4F complex, enables translation of TMG-SL RNAs. To investigate specific nematode proteins that might be involved in this translation effect, we first asked whether components of the nematode eIF4F complex were able to facilitate the enhanced translation of TMG-SL mRNAs. We depleted the eIF4F complex (typically eIF4E, eIF4G, and eIF4A) from *Ascaris* extracts by the use of m^7GTP-Sepharose affinity chromatography (10, 11). Western blot analysis of the depleted extract demonstrated that the majority of eIF4G and the three *Ascaris* eIF4E isoforms (eIF4E-1, eIF4E-3, and eIF4E-4) were depleted from the extracts (see Fig. S5 in the supplemental material). m^7GTP-Sepharose depletion of the extracts reduced translation competence to 1% of the nondepleted extract levels (data not shown). Reconstitution of the depleted extract with purified recombinant *Ascaris* eIF4E-3 and eIF4G, the two major components of eIF4F complex, increased translation 25-fold (Fig. 4A). Notably, eIF4E/G rescue of translation led to the translation profile observed with

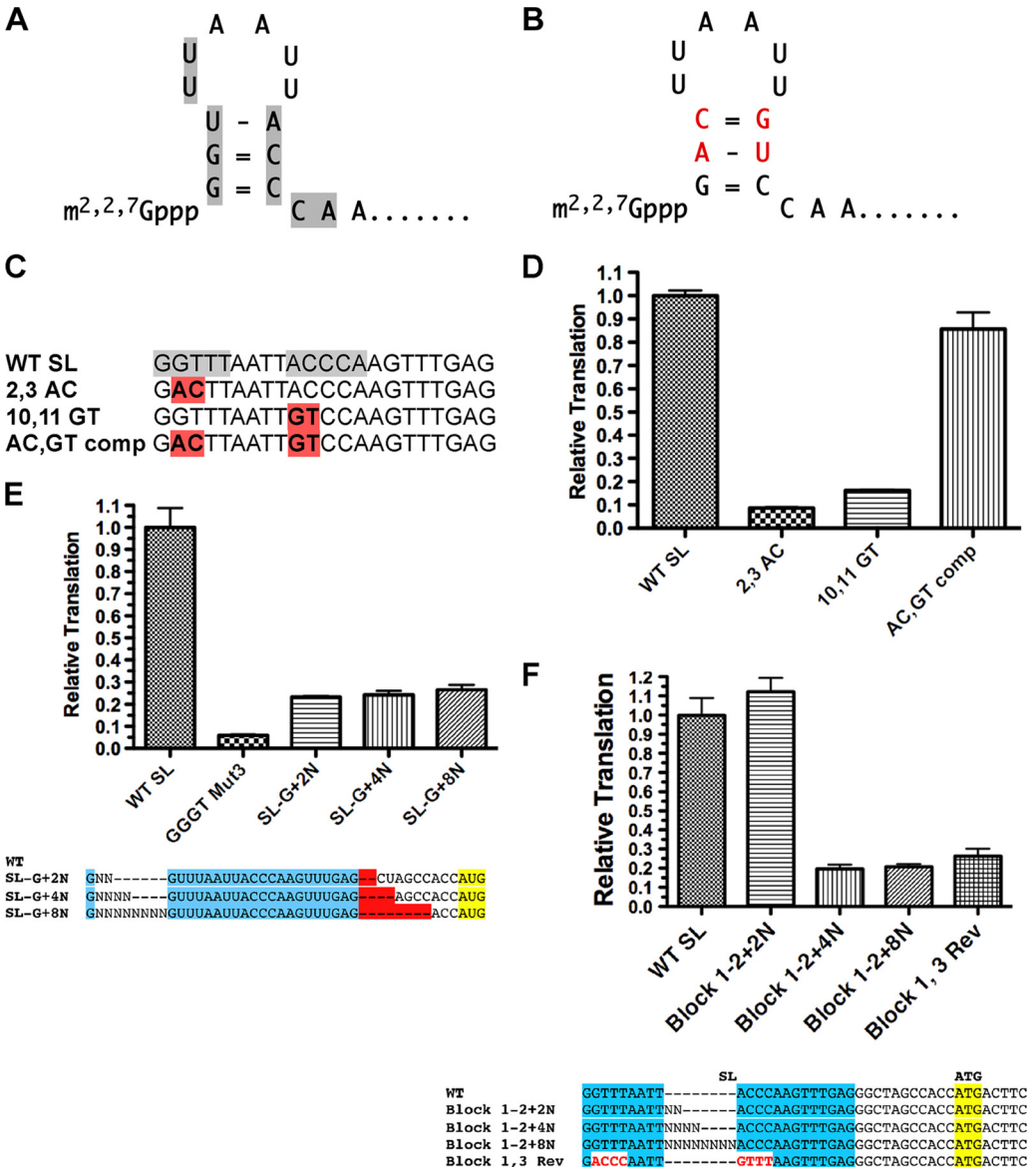

FIG. 3. Conserved SL sequences contribute to a 5′ stem-loop, and spacing of sequences within the SL are required for efficient translation of TMG-capped RNA. (A) Predicted 5′ stem-loop in the nematode SL1. Gray shading highlights the SL residues that contribute to the efficient translation of TMG-capped mRNAs. (B) Mutations in both stems of the SL that together would retain base pairing in the stem. Red-shaded residue sequences represent the mutated residues. (C) Designations and alignment of SL mutations that alter and reconstitute base pairing in the SL stem. Gray shading shows key sequences in the SL required for translation of TMG-capped RNA, and red shading denotes the nucleotide mutations. (D) Translation of RNAs with SL mutations that disrupt and then reconstitute the 5′ stem of the SL. (E) Block 1 sequences must be within 2 nt of the TMG to enable efficient translation of TMG-capped RNA. GGGT Mut3 is represented as described for Fig. 2C. Insertion mutations (e.g., +2N) were designed and compared with compensating deletions (e.g., −2N) following the SL to maintain a constant length in the 5′ UTR for translation comparisons. The plotted values were obtained by dividing the translation level of the "SL-G+XN" value by the "−XN" value (see Fig. S3 in the supplemental material for the illustration of the raw data). (F) The spacing of sequences between blocks 2 and 3 in the loop of the SL is important for efficient translation of TMG-capped RNA. Experiments were carried out as described for Fig. 1.

nondepleted extracts: significant translation of TMG-SL mRNA but limited translation of TMG-capped RNAs with SL mutations (Fig. 4A). 4E binding proteins and peptides derived from these proteins, namely, 4E binding peptide (4E-BP), compete with eIF4G for binding to eIF4E. Preincubation of *Ascaris* eIF4E/G complex with a 4E-BP peptide (RIIYDRKF LMECRNSPV) prior to their addition to the extract resulted in ~95% loss of reconstituted translation, indicating that both the complex and interaction between the two proteins were required for reconstitution (data not shown). Reconstitution of the m^{7}GTP-Sepharose-depleted *Ascaris* extract with wheat germ eIF4F complex (eIF4E, eIF4G, and eIF4A) did not result in the same effect for TMG-capped mRNAs (compare the ratio of WT SL/mutant SL for wheat germ [2.05] to that determined for *Ascaris* extracts [4.69]). These data suggest that the *Ascaris* eIF4E-3/G complex specifically contributed to the

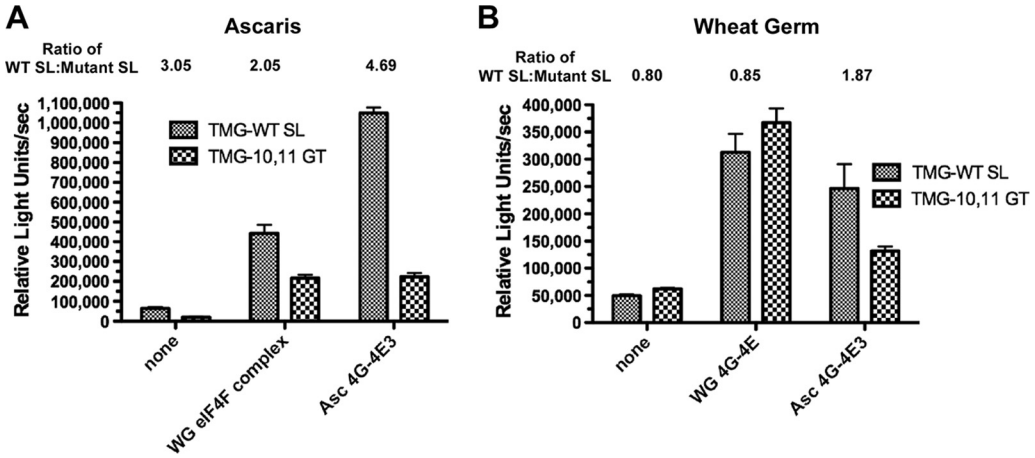

FIG. 4. The *Ascaris* eIF4E/G complex enabled efficient translation of TMG-capped RNA in the context of the WT spliced leader, but wheat germ eIF4F did not. (A) Depletion and reconstitution of *Ascaris* extracts with eIF4E/G. Note that reconstitution of eIF4F-depleted *Ascaris* extracts with *Ascaris* eIF4G/E recapitulated the "SL effect" and that efficient translation of a TMG-capped RNA required an intact SL. Note also that translation in nondepleted extracts resulted in a value of $\sim 7 \times 10^6$ relative light units/s. (B) Addition of eIF4E/G to wheat germ extracts. Note that in wheat germ translation extracts (B), translation of TMG capped mRNAs was very inefficient (<5% of m^7G capped RNAs; see Fig. 5). WG, wheat germ; Asc, *Ascaris*. WG eIF4F complex included wheat germ eIF4E, eIF4G, eIF4A, and eIF4B.

translation of TMG-SL mRNAs. We also added the *Ascaris* eIF4E-3/G complex to wheat germ extracts, for which levels of TMG-mediated translation of WT and mutant SL mRNAs are similar (Fig. 4B and Fig. 5A). However, the addition of *Ascaris* eIF4E-3/G complex increased translation of the TMG-capped WT SL mRNA nearly 2-fold (Fig. 4B). Together, these results suggest that the nematode eIF4E-3/G complex is one of the major determinants for the translational enhancement of TMG-capped mRNA by the SL stem-loop.

The contribution of these nematode initiation factors to the translation of TMG-capped RNAs suggests that the SL affects translation initiation. To confirm this, we examined the kinetics of translation and the formation of 80S ribosomes on TMG-capped RNAs. Time course translation experiments revealed that the difference between WT and mutant SL is a difference in the rate of translation (see Fig. S6A and B in the supplemental material), which indicates that the initiation processes for these two messages are different (34, 40). We also observed that more 80S ribosomes accumulate on the wild-type SL mRNA (see Fig. S6B in the supplemental material). Overall, these data confirm that the SL's enhancement of translation takes place at the initiation step. Unfortunately, using sucrose

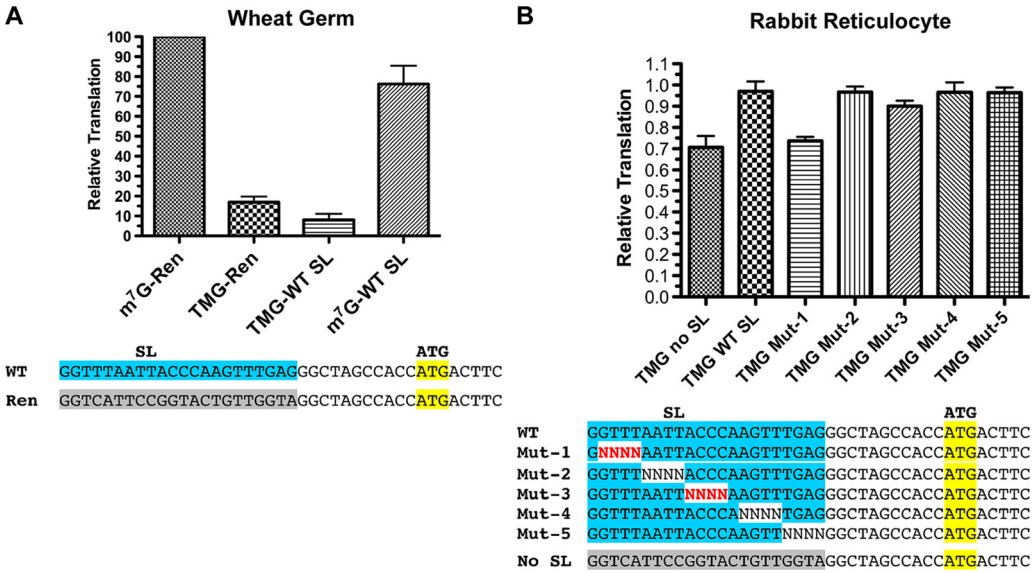

FIG. 5. SL-enhanced translation of TMG-capped RNAs was nematode specific. (A) The nematode spliced leader did not enhance translation of a TMG-capped Renilla reporter RNA in a wheat germ cell-free system. (B) The nematode spliced leader and mutations within the SL did not significantly enhance or affect translation of a TMG-capped Renilla reporter RNA in a heterologous rabbit reticulocyte translation system. Experiments were carried out as described for Fig. 1. Red-shaded characters represent random nucleotides whose presence led to a reduction in nematode translation of TMG-capped RNAs.

TABLE 1. Surface plasmon resonance data for Ascarid eIF4E-3/G complex with $m^{2,2,7}$G-capped wild-type SL, stem mutant SL, and stem compensatory mutant SL[a]

RNA	k_a	k_d	R_{max}	Residual SD	K_D (nM)
TMG-SL WT	3.27×10^5	1.09×10^{-3}	3,812	55.9	3.34
TMG-10,11 (GT)	2.88×10^5	1.32×10^{-3}	3,408	54.1	4.57
TMG-AC,GT	2.248×10^5	1.22×10^{-3}	3,788	56.0	5.45

[a] TMG-SL WT, $m^{2,2,7}$G-capped wild-type SL; TMG-10,11 (GT), stem mutant SL; TMG-AC,GT, stem compensatory mutant SL; k_a, rate constant association; k_d, rate constant dissociation; R_{max}, theoretical response maximum for channel; Residual SD, residual standard deviation; K_D, dissociation constant.

gradients with *Ascaris* extract, we were unable to resolve or trap 43S ribosome-loaded mRNAs, so we could not determine whether translation is affected before or after 43S complex loading.

SL does not affect the affinity of eIF4E/G for capped RNA. One hypothesis addressing how the nematode eIF4E/G complex works with the SL is that the SL stem-loop enhances eIF4E/G affinity for TMG-capped RNA. In order to examine this hypothesis, we used surface plasmon resonance (SPR) (32, 41) and different TMG-capped, polyadenylated small RNAs annealed to 5′ biotin-oligo(dT) immobilized on a streptavidin chip (see Materials and Methods). The recombinant *Ascaris* eIF4E-3/G complex showed the same relative affinity for the WT SL, the 10,11 GT Mut 3 SL, and the stem-loop compensatory AC,GT Mut SL RNAs (Table 1; also see Fig. S7A in the supplemental material). These binding data are in agreement with translation experiments demonstrating that the trimethylguanosine cap analog, which directly blocks capped-RNA recruitment to eIF4F (24), does not differentially inhibit TMG-capped messages with or without the SL (see Fig. S7B in the supplemental material). UV cross-linking experiments showed that recombinant *Ascaris* eIF4E-3 alone did not have an increased affinity for TMG-capped RNAs in the presence of the SL stem-loop (see Fig. S7C in the supplemental material). Similar experiments using filter binding and other SPR experiments confirmed these results (data not shown). Overall, these data suggest that the SL enhancement of translation does not involve the cap-binding affinity of the eIF4E/G complex for the RNA. In the wheat germ experiments represented by Fig. 4B, the *Ascaris* eIF4E-3/G complex provided a nearly 2-fold boost to TMG-WT SL mRNA translation. Thus, it remains possible that additional factors may be required to promote cap-binding or translation initiation.

Specificity of TMG-SL translation enhancement. The depletion and reconstitution of *Ascaris* extracts and addition of *Ascaris* eIF4E/G to wheat germ extracts suggest that this nematode complex is a key determinant in the translation enhancement of TMG-capped SL mRNAs and that the enhanced translation would be observed only in nematode extracts. We therefore asked whether the spliced leader sequence specifically enhanced translation of TMG-capped mRNAs in heterologous translation systems. mRNAs in eukaryotes typically have a m^7G cap, and eIF4E, the cap-binding protein required for cap-dependent translation initiation, has a low affinity for the TMG cap (35, 43, 54). Translation in wheat germ extracts is dependent on the presence of cap; however, translation in rabbit reticulocytes is quite promiscuous, enabling some translation of TMG-capped RNAs (6). As shown in Fig. 5, the SL sequence does not play the same role in enhancing translation in other eukaryotic translation systems. Thus, the effect of the SL on TMG-capped translation is specific to the nematode translation system and is enabled by nematode *trans*-acting factors, including eIF4E/G.

Nematode SL core sequences are conserved. The SL1 sequence is highly conserved in rhabditid nematodes (Fig. 6A). A second spliced leader (SL2) and a number of related variants are present in *Caenorhabditis elegans* (19, 42). Alignment of *Ascaris* SL1, *C. elegans* SL2 (Fig. 6B), and several additional SL variants in nematodes (Fig. 6C) demonstrated that the key SL sequences are conserved (15). Notably, the conservation of the SL stem is supported by the existence of covariations in some of the SLs. For example, in Pp2f SL2, covariation in nt 3 and 9 maintains the stem structure. Similar covariations are also found in Bm1a SL1 and Ppa SL2a (Fig. 6A, C, and D).

The major differences between SL1 and SL2 are represented by the nucleotides in blocks 2 and 5 (Fig. 6C). We examined several of these variant SLs and hybrid SLs in the *Ascaris in vitro* translation system (see Fig. S8A in the supplemental material). These analyses demonstrated that a hybrid SL that used the 5′ end of SL2 with the 3′ end of SL1 enabled efficient translation of the TMG cap (see 5′ SL2-SL1 3′ in Fig. S8A in the supplemental material) and that the 3′ end of the SL plays a minimal role in facilitating translation of the TMG cap (see Fig. S8A in the supplemental material). Overall, these data suggest that the residues (GGUUUNNNNACCCANNNNN NNN) are important for efficient translation of TMG-capped mRNAs not only in *Ascaris* species but also in many divergent nematode species.

In all spliced leaders identified, the three 3′-most nucleotides are invariably purines. We substituted three Ts for these purines but observed no effect on translation (see SL-TTT in Fig. S8A in the supplemental material). Recently, variant spliced leaders in what is considered a basal nematode lineage, *Trichinella spiralis*, were described (38). In contrast to the high conservation of SL1- and SL2-like sequences observed in other nematodes, *Trichinella* SLs are numerous and divergent. However, several of the spliced leaders (Tp1, Tp2, and Tp3) have portions of the conserved blocks that we have identified as important. These regions can contribute to the enhanced translation of TMG-capped mRNAs in *Ascaris* extracts (see Fig. S8B in the supplemental material).

DISCUSSION

Efficient translation of a TMG-capped mRNA in the *Ascaris* nematode requires the associated 22-nt *trans*-spliced SL1 sequence (5, 25, 29). We refer to this phenomenon as the "SL effect." Here, we define the nucleotides within the highly conserved nematode SL1 spliced leader (nucleotides 1 to 5 and 10 to 14 [GGUUUNNNNACCCANNNNNNNN]) required for the SL effect (Fig. 1 and 2). The identified core nucleotides contribute to a functionally required stem-loop at the 5′ end of the SL (Fig. 3). The contribution of the SL to efficient translation is specific to both the TMG cap and nematodes (Fig. 1A and 5). Several lines of evidence demonstrate that the nematode eIF4E-3/G complex is a critical determinant for the SL effect. First, depletion of the complex from nematode ex-

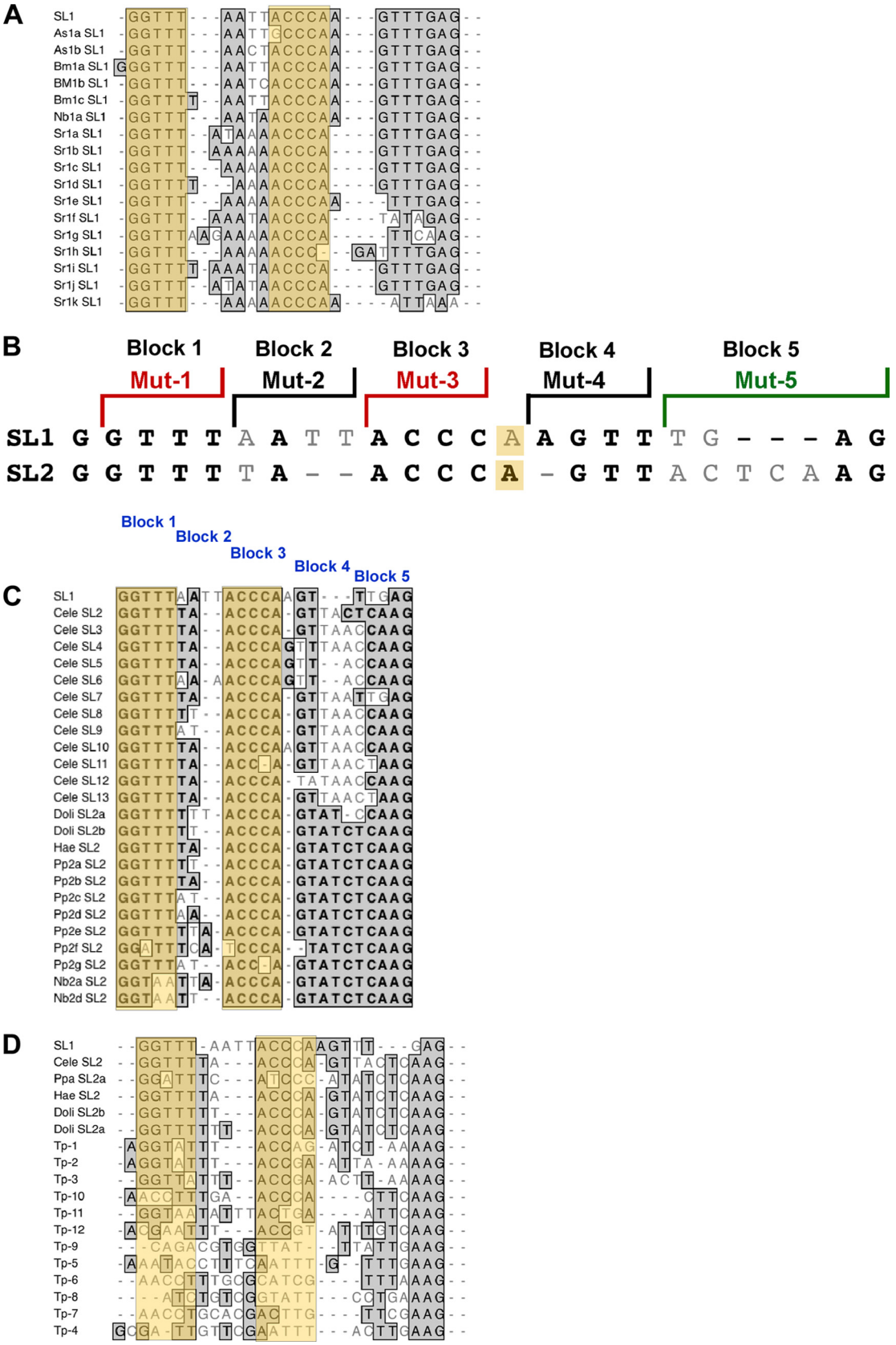

FIG. 6. Alignment and sequence conservation of nematode spliced leaders identified key SL regions associated with efficient translation of the TMG cap. (A) Rhabditid SL1 sequences. (B) Comparison of *C. elegans* SL1 and the primary SL2 sequence, illustrating the conserved sequences and regions mutated as shown in previous figures. (C) Rabditid SL2-like sequences. (D) Diversity of SL sequences in nematodes. Bold or shaded sequences represent identical residues, light gray residues represent variants, and dashes represent spacing to facilitate alignments. The orange shading depicts blocks 1 and 3 of the spliced leader. Nucleotide 14 is included here in block 3.

tracts and its reconstitution with recombinant nematode eIF4E/G complex, but not the wheat germ complex, demonstrates the SL effect (Fig. 4A and B). Second, the SL effect is not observed in wheat germ translation extracts. Third, the addition of the nematode eIF4E/G complex, but not the wheat germ complex, to wheat germ extracts leads to the SL effect in wheat germ extracts. Overall, these data demonstrate that the nematode eIF4E/G complex works with the SL stem-loop and associated sequences to facilitate nematode translation of TMG-capped mRNAs.

Nematode SL stem-loop required for efficient translation of TMG-capped RNA. Spacing of nucleotides within SL1 is important, with a minimal distance between the TMG cap and block 1 required (Fig. 3E and F). The length of the loop plays a role in translation, as insertion of more than 2 nt into the loop abrogates the enhancement of translation (Fig. 3F). The loop can be reduced by 2 nt, as illustrated by SL2, which is translated efficiently. Mutations on both sides of the stem that restore base pairing indicate that the stem is required for enhancing translation. The stem mutations introduced in this study were all transitions and thus maintained some character of the bases. While the structure is required, there also may be some sequence requirements. In addition, nucleotides within the loop and immediately 3′ of the stem also facilitate translation of TMG-capped RNAs (Fig. 3). The second guanine nucleotide of the TMG cap is also required for efficient TMG-capped RNA translation (Fig. 2B). A 3-bp stem would be predicted to be quite weak, so we hypothesize that the trimethylated guanosine cap may physically interact with the cytosine or adenosine immediately 3′ of the stem or the RNA structure to stabilize the stem and/or contribute to a novel structure. Overall, it is likely that the stem-loop structure, a higher-order structure, or its stability is dependent on some attribute specific to the TMG cap because m^7G-capped RNA translation is not enhanced by the SL. Interestingly, high-throughput RNA sequencing of *Ascaris* mRNAs demonstrated that the majority of the mRNA sequences that extend 5′ to the SL stop predominantly at the C that is immediately downstream of the stem (data not shown). These data further suggest that a structural element is present at the 5′ end of the SL.

Mechanisms through which the eIF4E/4G complex might facilitate translation initiation. Recognition of the mRNA cap by eIF4E (and recruitment of the ribosome through eIF4G in the eIF4F complex) is a rate-limiting step of translation (13, 37, 50). In contrast with most eukaryotic eIF4Es, *Ascaris* eIF4E-3 and several *C. elegans* eIF4Es recognize the TMG cap in addition to the m^7G cap (20, 22, 25). Addition of *Ascaris* eIF4E-3 directly to translation extracts or m^7GTP-Sepharose-depleted extracts did not significantly enhance translation or show the "SL effect." We previously reported (using UV cross-linking) that (i) recombinant nematode eIF4E bound only to capped RNA and (ii) binding to the TMG cap appeared greater when the SL was present (25). However, efforts to further characterize and quantify the potential interaction between eIF4E-3 and TMG-SL RNA by the use of filter binding assays, surface plasmon resonance, and other approaches did not demonstrate that the core residues, GGUUUNNNNACCCANNNNNNNN, play a large role in enhancing cap binding (see Fig. S7B in the supplemental material). Overall, these data suggest that while nematode eIF4E may recognize the TMG cap, the SL and nematode eIF4G may be necessary to either stabilize the complex or enhance recruitment of the 43S complex for translation initiation. Therefore, it would be predicted that in the absence of the SL or with mutations in the SL, ribosome recruitment would be less efficient. The kinetics of translation and the formation of 80S ribosomes on wild-type and mutant SL mRNAs demonstrate that the SL does indeed enhance translation initiation (see Fig. S6 in the supplemental material). Experiments using cap analogs as competitive inhibitors of translation suggest the SL may contribute to translation of TMG-capped RNAs after the initial cap-binding step (see Fig. S7A in the supplemental material).

The data presented here suggest that the stem-loop structure does not increase eIF4E/4G's affinity for the capped messages (Fig. 4C and D). One possible model to explain the SL requirement for TMG-capped RNA translation is that the nematode eIF4G has adapted to interact, directly or indirectly, with the SL sequence to enhance recruitment of the 43S complex to the mRNA, form a stable 48S complex on the mRNA, enhance its scanning, or join to the 60S subunit. eIF4G is a known RNA binding protein, and interactions between eIF4E and eIF4G upon binding to the cap could enable conformation changes and interaction with the SL to facilitate translation (1, 14, 18, 21, 40, 53). A great deal of sequence and functional diversity between eIF4Gs exists (11, 13). Overall, *Ascaris* eIF4G shows only 15% identity and 12% similarity to wheat germ eIF4G and 21% identity and 14% similarity to human eIF4GI (see Fig. S1 in the supplemental material). While there is higher similarity in the core, central domain, it is difficult to identify regions of *Ascaris* eIF4G that might be unique and contribute to the SL effect. Experiments are under way to evaluate RNA binding of *Ascaris* eIF4G to the RNA stem-loop on *trans*-spliced mRNAs.

The specific spacing requirements necessary for efficient translation, including the distance from the TMG cap to the stem and size of the loop, suggest that a specific binding site is likely to be used by proteins. Our efforts to identify a *trans*-acting protein that binds TMG-SL RNA compared to m^7G-SL RNA or the TMG cap alone have not yet identified any auxiliary proteins (data not shown). We were unable to detect recruitment or scanning of the 43S complex by the use of a variety of approaches and inhibitors in sucrose gradient analysis of translation extracts. Thus, we currently cannot determine whether the SL and eIF4E-3/G enhance recruitment of the 43S complex, increase ribosome scanning, or enhance formation of the 80S ribosome. Additional studies will be required to further define the detailed mechanism and contribution of nematode eIF4E/G in the enhancement of translation of TMG-capped mRNA by the SL.

Conservation of key SL1 nucleotides in other nematode spliced leaders. *C. elegans* has a second spliced leader, SL2 (with a number of variants) (19, 42). Orthologous SL2 sequences are also present in several other nematodes (Fig. 6C). Alignment of these SL2-like sequences illustrates that the most highly conserved regions consist of the sequences defined here (GGUUUNNNNACCCANNNNNNNN) that exert the greatest effect in enhancing translation of TMG-capped RNA. We show here that the *C. elegans* SL2 sequence is efficiently translated in the *Ascaris* cell-free system (see Fig. S8 in the supplemental material).

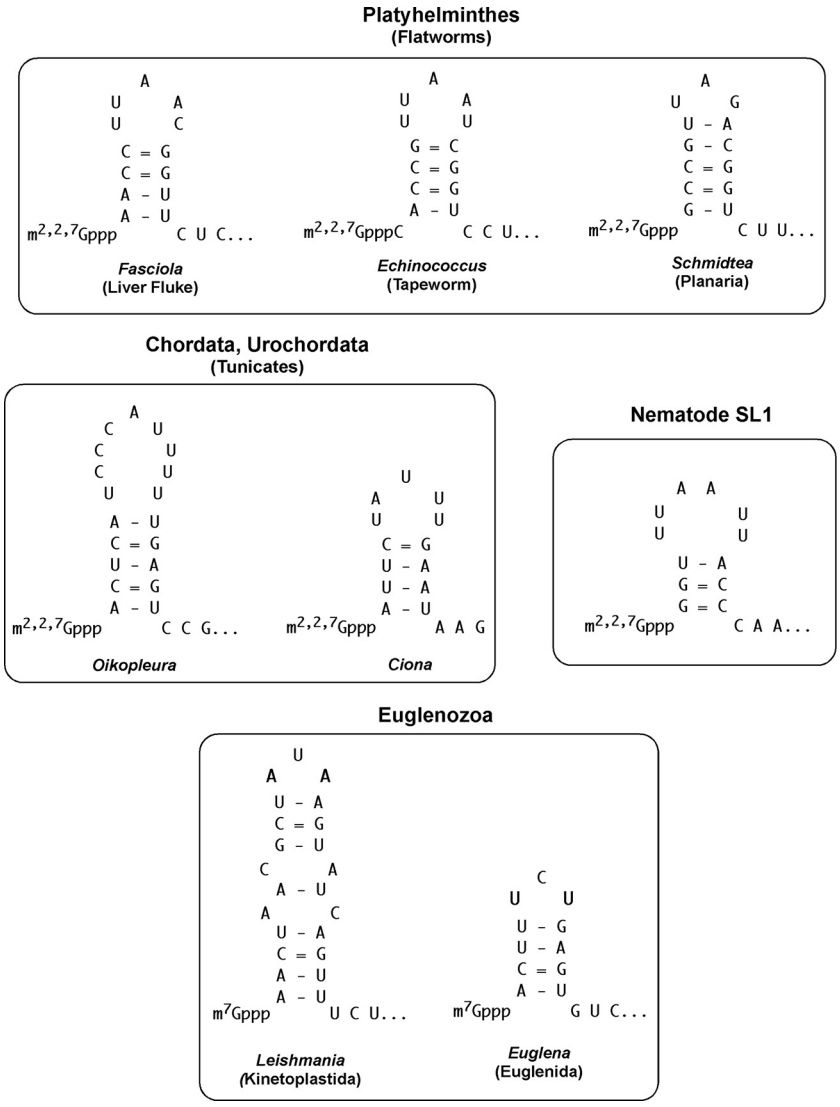

FIG. 7. Potential stem-loop structures adjacent to the cap in phylogenetically divergent spliced leaders. Note that while many SLs have been predicted to have a stem-loop adjacent to the cap, the sequences contributing to the stem are divergent. The nematode SL1 stem-loop is shown for comparison. Representatives of 3 separate classes of flatworms (*Turbellaria*, *Trematoda*, and *Cestoda*) and representatives of 2 different classes of the *Euglenozoa* (*Kinetoplastida* and *Euglenida*) are illustrated. Sequences are derived as follows: *Schmidtea mediterranea* (55), *Fasciola hepatica* (7), *Echinococcus multilocularis* (4), *Oikopleura dioica* (12), *Ciona intestinalis* (48), *Leishmania* spp. (34), and *Euglena gracilis* (45).

Sequence alignments demonstrate that the 3′ end of the nematode SL exhibits considerable sequence variation (Fig. 6), and both mutation studies and translation assays of alternative and hybrid SL sequences on reporter RNAs show that these sequences do not play a significant role in translation (Fig. 1; see also Fig. S8 in the supplemental material). Although the final three nucleotides in all nematode SLs are purines, replacement of these purines with pyrimidines had little effect on translation. Many SLs are *trans*-spliced immediately upstream of the AUG mRNA coding region (25). In this context, these purines would contribute key nucleotides to the −1 to −3 in the context of eukaryotic initiation, where purines are known to play an important role in translation.

Recently, a number of highly divergent SLs in species of *Trichinella*, which is considered a basal member of the nematode lineage, were described (38). Interestingly, several key residues in blocks 1 and 3 of SL1 and SL2 in the rhabditid lineage are conserved in a few of the variable *Trichinella* spliced leaders. While the tested *Trichinella* spliced leaders supported TMG translation in the *Ascaris* cell-free system, they were at best only ~50% as efficient (see Fig. S4 in the supplemental material). If the lineage is basal, the selection and conservation of these core sequences in blocks 1 and 3 may have given rise to SL1 and SL2 in some lineages. Alternatively, the sequence divergence in *Trichinella* SLs may indicate that this nematode lineage is highly derived.

The highly conserved rhabditid nematode SL1 sequence (see Fig. 6A) is a core, internal promoter element for transcription of SL RNA genes but is not a key element for the *trans*-splicing reaction (9, 16, 31). Here we show that the SL1 sequence conservation is also related to an important role in contributing to the overall translation of TMG-capped mRNAs. There-

fore, at least two functional constraints maintain SL1 sequence conservation.

Role of key SL residues in vivo. Maroney et al. first demonstrated that a 10-nt substitution (nt 7 to 16) within the SL sequence led to a decrease in translation in an *Ascaris* cell-free system (29). Ferguson and Rothman demonstrated that some sequences within the SL1 were critical for *C. elegans* embryonic survival, but their potential role in posttranscriptional gene expression was not defined (9). Interestingly, they showed that alterations within the core sequences identified here or altered spacing between these blocks was not able to rescue embryonic lethality. These alterations did not affect SL RNA expression or the *trans*-splicing reaction and therefore likely altered the postsplicing function of SL1. Nucleotide substitutions downstream of the ACCCA were still able to rescue embryonic lethality, which is consistent with our translation data. Notably, the SL1 regions required for *C. elegans* embryonic development correspond to the regions we have identified here as necessary for optimal translation of TMG-capped RNA in our cell-free system. Here we reveal the underlying mechanism for the requirement of these SL regions.

Evolution of *trans* splicing and the SL effect. Efficient translation of TMG-capped mRNA in vivo or in vitro requires the spliced leader. This suggests that optimal translation of TMG-capped mRNAs evolved in the context of the downstream SL and that the initial appearance of *trans* splicing likely would have produced mRNAs that were not efficiently translated (5, 25). *trans*-spliced mRNAs are not translated more efficiently and the RNAs are not more stable in nematode embryos compared to m^7G-capped non-*trans*-spliced mRNAs (5, 25). Therefore, the introduction and maintenance of *trans* splicing were most likely not related to an advantage in translation or mRNA stability but to some other advantage provided by this process. A number of *trans*-spliced metazoan mRNAs (apparently not the majority) are derived from polycistronic transcripts, and thus *trans* splicing contributes to their resolution into monocistronic mRNAs. If polycistronic transcripts were initially present in nematode lineages, *trans* splicing must have evolved either before or simultaneously with these atypical eukaryotic transcription units or else some alternate mechanism of translation initiation was present (perhaps internal ribosome entry sites) to enable translation of the proteins from these polycistronic transcripts.

SL stem-loops. We examined other metazoan spliced leaders for the presence of a stem-loop adjacent to the cap. Indeed, many of the spliced leaders can be predicted to form a stem-loop adjacent to the cap (Fig. 7). Thus, the presence of an SL stem-loop adjacent to the cap may be a common feature of *trans* splicing.

Conclusions. We have defined elements within the nematode SL1 spliced leader that form a stem-loop and the eIF4F complex required for efficient translation of TMG-capped RNAs generated by *trans* splicing. While sequences within the 5′ UTR of eukaryotic mRNAs are known to have a modulating effect on translation (most often negative), our studies demonstrate the importance of specific elements in the 5′ UTR and adaptation in the eIF4F complex necessary for optimal cap-dependent translation.

ACKNOWLEDGMENTS

We are particularly grateful to Karen Browning for helpful discussions and for generously providing wheat germ translation extracts and eIF4F complex. We thank Tom Evans, Tom Blumenthal, Jeffrey Kieft, Tim Nilsen, and members of the Davis laboratory for their comments on the manuscript.

This work was supported by NIH grant AI49558 to R.E.D. and by grants from the Howard Hughes Medical Institute grant (55005604) and National Science Support Project 2008-2010 no. PBZ-MNiSW-07/1/2007 to E.D.

REFERENCES

1. **Berset, C., A. Zurbriggen, S. Djafarzadeh, M. Altmann, and H. Trachsel.** 2003. RNA-binding activity of translation initiation factor eIF4G1 from Saccharomyces cerevisiae. RNA **9:**871–880.
2. **Blumenthal, T.** 25 June 2005, posting date. Trans-splicing and operons. *In* The *C. elegans* Research Community (ed.), WormBook. doi/10.1895/wormbook.1.5.1. http://www.wormbook.org/.
3. **Bonen, L.** 1993. Trans-splicing of pre-mRNA in plants, animals, and protists. FASEB J. **7:**40–46.
4. **Brehm, K., K. Jensen, and M. Frosch.** 2000. mRNA trans-splicing in the human parasitic cestode Echinococcus multilocularis. J. Biol. Chem. **275:**38311–38318.
5. **Cheng, G., L. Cohen, C. Mikhli, M. Jankowska-Anyszka, J. Stepinski, E. Darzynkiewicz, and R. E. Davis.** 2007. In vivo translation and stability of trans-spliced mRNAs in nematode embryos. Mol. Biochem. Parasitol. **153:**95–106.
6. **Darzynkiewicz, E., J. Stepinski, I. Ekiel, Y. Jin, D. Haber, T. Sijuwade, and S. M. Tahara.** 1988. Beta-globin mRNAs capped with m7G, m2.7(2)G or m2.2.7(3)G differ in intrinsic translation efficiency. Nucleic Acids Res. **16:**8953–8962.
7. **Davis, R. E., H. Singh, C. Botka, C. Hardwick, M. Ashraf el Meanawy, and J. Villanueva.** 1994. RNA trans-splicing in Fasciola hepatica. Identification of a spliced leader (SL) RNA and SL sequences on mRNAs. J. Biol. Chem. **269:**20026–20030.
8. **Douris, V., M. J. Telford, and M. Averof.** 25 November 2009, posting date. Evidence for multiple independent origins of trans-splicing in Metazoa. Mol. Biol. Evol. [Epub ahead of print.]
9. **Ferguson, K. C., and J. H. Rothman.** 1999. Alterations in the conserved SL1 trans-spliced leader of Caenorhabditis elegans demonstrate flexibility in length and sequence requirements in vivo. Mol. Cell. Biol. **19:**1892–1900.
10. **Gallie, D. R.** 2007. Use of in vitro translation extract depleted in specific initiation factors for the investigation of translational regulation. Methods Enzymol. **429:**35–51.
11. **Gallie, D. R., and K. S. Browning.** 2001. eIF4G functionally differs from eIFiso4G in promoting internal initiation, cap-independent translation, and translation of structured mRNAs. J. Biol. Chem. **276:**36951–36960.
12. **Ganot, P., T. Kallesoe, R. Reinhardt, D. Chourrout, and E. M. Thompson.** 2004. Spliced-leader RNA trans splicing in a chordate, Oikopleura dioica, with a compact genome. Mol. Cell. Biol. **24:**7795–7805.
13. **Gingras, A.-C., B. Raught, and N. Sonenberg.** 1999. eIF4 initiation factors: effectors of mRNA recruitment to ribosomes and regulators of translation. Annu. Rev. Biochem. **68:**913–963.
14. **Gross, J. D., N. J. Moerke, T. von der Haar, A. A. Lugovskoy, A. B. Sachs, J. E. McCarthy, and G. Wagner.** 2003. Ribosome loading onto the mRNA cap is driven by conformational coupling between eIF4G and eIF4E. Cell **115:**739–750.
15. **Guiliano, D. B., and M. L. Blaxter.** 2006. Operon conservation and the evolution of trans-splicing in the phylum Nematoda. PLoS Genetics **2:**e198.
16. **Hannon, G. J., P. A. Maroney, D. G. Ayers, J. D. Shambaugh, and T. W. Nilsen.** 1990. Transcription of a nematode trans-spliced leader RNA requires internal elements for both initiation and 3′ end-formation. EMBO J. **9:**1915–1921.
17. **Hastings, K. E.** 2005. SL trans-splicing: easy come or easy go? Trends Genet. **21:**240–247.
18. **Hinton, T. M., M. J. Coldwell, G. A. Carpenter, S. J. Morley, and V. M. Pain.** 2007. Functional analysis of individual binding activities of the scaffold protein eIF4G. J. Biol. Chem. **282:**1695–1708.
19. **Huang, X. Y., and D. Hirsh.** 1989. A second trans-spliced RNA leader sequence in the nematode Caenorhabditis elegans. Proc. Natl. Acad. Sci. U. S. A. **86:**8640–8644.
20. **Jankowska-Anyszka, M., B. J. Lamphear, E. J. Aamodt, T. Harrington, E. Darzynkiewicz, R. Stolarski, and R. E. Rhoads.** 1998. Multiple isoforms of eukaryotic protein synthesis initiation factor 4E in C. elegans can distinguish between mono- and trimethylated mRNA cap structures. J. Biol. Chem. **273:**10538–10542.
21. **Kaye, N. M., K. J. Emmett, W. C. Merrick, and E. Jankowsky.** 2009. Intrinsic RNA binding by the eukaryotic initiation factor 4F depends on a minimal RNA length but not on the m7G cap. J. Biol. Chem. **284:**17742–17750.
22. **Keiper, B. D., B. J. Lamphear, A. M. Deshpande, M. Jankowska-Anyszka,**

E. J. Aamodt, T. Blumenthal, and R. E. Rhoads. 2000. Functional characterization of five eIF4E isoforms in *Caenorhabditis elegans*. J. Biol. Chem. **275:**10590–10596.
23. **Kozak, M.** 2005. Regulation of translation via mRNA structure in prokaryotes and eukaryotes. Gene **361:**13–37.
24. **Kozak, M.** 1991. A short leader sequence impairs the fidelity of initiation by eukaryotic ribosomes. Gene Expr. **1:**111–115.
25. **Lall, S., C. C. Friedman, M. Jankowska-Anyszka, J. Stepinski, E. Darzynkiewicz, and R. E. Davis.** 2004. Contribution of trans-splicing, 5′-leader length, cap-poly(A) synergism, and initiation factors to nematode translation in an Ascaris suum embryo cell-free system. J. Biol. Chem. **279:**45573–45585.
26. **Liang, X. H., A. Haritan, S. Uliel, and S. Michaeli.** 2003. trans and cis splicing in trypanosomatids: mechanism, factors, and regulation. Eukaryot. Cell **2:**830–840.
27. **Liou, R. F., and T. Blumenthal.** 1990. *trans*-spliced *Caenorhabditis elegans* mRNAs retain trimethylguanosine caps. Mol. Cell. Biol. **10:**1764–1768.
28. **Marlétaz, F., A. Gilles, X. Caubit, Y. Perez, C. Dossat, S. Samain, G. Gyapay, P. Wincker, and Y. Le Parco.** 2008. Chaetognath transcriptome reveals ancestral and unique features among bilaterians. Genome Biol. **9:**R94.
29. **Maroney, P. A., J. A. Denker, E. Darzynkiewicz, R. Laneve, and T. W. Nilsen.** 1995. Most mRNAs in the nematode Ascaris lumbricoides are trans-spliced: a role for spliced leader addition in translational efficiency. RNA **1:**714–723.
30. **Maroney, P. A., G. J. Hannon, and T. W. Nilsen.** 1990. Transcription and cap trimethylation of a nematode spliced leader RNA in a cell-free system. Proc. Natl. Acad. Sci. U. S. A. **87:**709–713.
31. **Maroney, P. A., G. J. Hannon, J. D. Shambaugh, and T. W. Nilsen.** 1991. Intramolecular base pairing between the nematode spliced leader and its 5′ splice site is not essential for trans-splicing in vitro. EMBO J. **10:**3869–3875.
32. **McCarthy, J. E., S. Marsden, and T. von der Haar.** 2007. Biophysical studies of the translation initiation pathway with immobilized mRNA analogs. Methods Enzymol. **430:**247–264.
33. **Merino, E. J., K. A. Wilkinson, J. L. Coughlan, and K. M. Weeks.** 2005. RNA structure analysis at single nucleotide resolution by selective 2′-hydroxyl acylation and primer extension (SHAPE). J. Am. Chem. Soc. **127:**4223–4231.
34. **Miller, S. I., S. M. Landfear, and D. F. Wirth.** 1986. Cloning and characterization of a Leishmania gene encoding a RNA spliced leader sequence. Nucleic Acids Res. **14:**7341–7360.
35. **Niedzwiecka, A., E. Darzynkiewicz, and R. Stolarski.** 2004. Thermodynamics of mRNA 5′ cap binding by eukaryotic translation initiation factor eIF4E. Biochemistry **43:**13305–13317.
36. **Nilsen, T. W.** 1997. Trans-splicing, p. 310–334. *In* A. R. Krainer (ed.), Frontiers in molecular biology: eukaryotic mRNA processing. IRL Press, Oxford, United Kingdom.
37. **Pestova, T. V., J. R. Lorsch, and C. U. T. Hellen.** 2007. The mechanism of translation initiation in eukaryotes, p. 87–128. *In* M. B. Mathews, N. Sonenberg, and J. W. B. Hershey (ed.), Translational control in biology and medicine. Cold Spring Harbor Press, Woodbury, NY.
38. **Pettitt, J., B. Muller, I. Stansfield, and B. Connolly.** 2008. Spliced leader trans-splicing in the nematode Trichinella spiralis uses highly polymorphic, noncanonical spliced leaders. RNA **14:**760–770.
39. **Pouchkina-Stantcheva, N. N., and A. Tunnacliffe.** 2005. Spliced-leader RNA mediated trans-splicing in phylum Rotifera. Mol. Biol. Evol. **22:**1482–1489.
40. **Prévôt, D., D. Decimo, C. H. Herbreteau, F. Roux, J. Garin, J. L. Darlix, and T. Ohlmann.** 2003. Characterization of a novel RNA-binding region of eIF4GI critical for ribosomal scanning. EMBO J. **22:**1909–1921.
41. **Ptushkina, M., T. von der Haar, M. M. Karim, J. M. Hughes, and J. E. McCarthy.** 1999. Repressor binding to a dorsal regulatory site traps human eIF4E in a high cap-affinity state. EMBO J. **18:**4068–4075.
42. **Ross, L. H., J. H. Freedman, and C. S. Rubin.** 1995. Structure and expression of novel spliced leader RNA genes in Caenorhabditis elegans. J. Biol. Chem. **270:**22066–22075.
43. **Rutkowska-Wlodarczyk, I., J. Stepinski, M. Dadlez, E. Darzynkiewicz, R. Stolarski, and A. Niedzwiecka.** 2008. Structural changes of eIF4E upon binding to the mRNA 5′ monomethylguanosine and trimethylguanosine Cap. Biochemistry **47:**2710–2720.
44. **Sonenberg, N., and A. G. Hinnebusch.** 2009. Regulation of translation initiation in eukaryotes: mechanisms and biological targets. Cell **136:**731–745.
45. **Tessier, L. H., M. Keller, R. L. Chan, R. Fournier, J. H. Weil, and P. Imbault.** 1991. Short leader sequences may be transferred from small RNAs to pre-mature mRNAs by trans-splicing in Euglena. EMBO J. **10:**2621–2625.
46. **Thomas, J. D., R. C. Conrad, and T. Blumenthal.** 1988. The C. elegans trans-spliced leader RNA is bound to Sm and has a trimethylguanosine cap. Cell **54:**533–539.
47. **Ullu, E., and T. W. Nilsen.** 1995. Molecular biology of protozoan and helminth parasites, p. 1–17. *In* J. Marr and M. Muller (ed.), Biochemistry of parasitic organisms and its molecular foundations. Academic Press, London, United Kingdom.
48. **Vandenberghe, A. E., T. H. Meedel, and K. E. Hastings.** 2001. mRNA 5′-leader trans-splicing in the chordates. Genes Dev. **15:**294–303.
49. **Van Doren, K., and D. Hirsh.** 1990. mRNAs that mature through trans-splicing in Caenorhabditis elegans have a trimethylguanosine cap at their 5′ termini. Mol. Cell. Biol. **10:**1769–1772.
50. **von der Haar, T., J. D. Gross, G. Wagner, and J. E. McCarthy.** 2004. The mRNA cap-binding protein eIF4E in post-transcriptional gene expression. Nat. Struct. Mol. Biol. **11:**503–511.
51. **Wilkinson, K. A., E. J. Merino, and K. M. Weeks.** 2006. Selective 2′-hydroxyl acylation analyzed by primer extension (SHAPE): quantitative RNA structure analysis at single nucleotide resolution. Nat. Protoc. **1:**1610–1616.
52. **Wu, L., J. Fan, and J. G. Belasco.** 2006. MicroRNAs direct rapid deadenylation of mRNA. Proc. Natl. Acad. Sci. U. S. A. **103:**4034–4039.
53. **Yanagiya, A., Y. V. Svitkin, S. Shibata, S. Mikami, H. Imataka, and N. Sonenberg.** 2009. Requirement of RNA binding of mammalian eukaryotic translation initiation factor 4GI (eIF4GI) for efficient interaction of eIF4E with the mRNA cap. Mol. Cell. Biol. **29:**1661–1669.
54. **Yoffe, Y., J. Zuberek, M. Lewdorowicz, Z. Zeira, C. Keasar, I. Orr-Dahan, M. Jankowska-Anyszka, J. Stepinski, E. Darzynkiewicz, and M. Shapira.** 2004. Cap-binding activity of an eIF4E homolog from Leishmania. RNA **10:**1764–1775.
55. **Zayas, R. M., T. D. Bold, and P. A. Newmark.** 2005. Spliced-leader trans-splicing in freshwater planarians. Mol. Biol. Evol. **22:**2048–2054.
56. **Zhang, H., Y. Hou, L. Miranda, D. A. Campbell, N. R. Sturm, T. Gaasterland, and S. Lin.** 2007. Spliced leader RNA trans-splicing in dinoflagellates. Proc. Natl. Acad. Sci. U. S. A. **104:**4618–4623.

Supplementary Material

In previous work, we demonstrated that 3' → 5' RNA decay followed by scavenger decapping of the resulting cap was very active in our translation extracts (1). In contrast, direct mRNA decapping occurred at very low levels in the translation extracts, and thus 5' → 3' decay played a very minor role in mRNA decay compared to the 3' → 5' RNA decay pathway. To rule out that the mutations in blocks 1 or 3 led to differential RNA decapping of RNA that might contribute to the differences in translation observed, we examined the rate of decay of 5' monophosphate RNAs (the products of RNA decapping) and compared the amounts of decapped RNAs derived from wild type or mutant SL mRNAs that accumulated during translation in the extracts (see Materials and Methods). 5' monophosphate RNAs were significantly less stable than TMG-capped RNAs in the extracts indicating that decapped RNAs are not likely to accumulate in the extracts (Supplementary Figure 2A). In addition, comparison of the wild-type and mutant RNAs at different time points during translation did not show any differences in the levels of decapped or 5' monophosphate RNAs for these RNAs during the translation reactions (Supplementary Figure 2B). Overall, these data suggest that differential mRNA decapping of wild-type vs mutant SL 1 and 3 is not an explanation for the reduction in translation observed for the mutations in the SLs.

References

1. **Cohen, L. S., C. Mikhli, C. Friedman, M. Jankowska-Anyszka, J. Stepinski, E. Darzynkiewicz, and R. E. Davis.** 2004. Nematode m7GpppG and m3(2,2,7)GpppG decapping: activities in Ascaris embryos and characterization of C. elegans scavenger DcpS. RNA **10:**1609-24.
2. **Lall, S., C. C. Friedman, M. Jankowska-Anyszka, J. Stepinski, E. Darzynkiewicz, and R. E. Davis.** 2004. Contribution of trans-splicing, 5' -leader length, cap-poly(A) synergism, and initiation factors to nematode translation in an Ascaris suum embryo cell-free system. J Biol Chem **279:**45573-85.
3. **Merino, E. J., K. A. Wilkinson, J. L. Coughlan, and K. M. Weeks.** 2005. RNA structure analysis at single nucleotide resolution by selective 2'-hydroxyl acylation and primer extension (SHAPE). J Am Chem Soc **127:**4223-31.
4. **Wilkinson, K. A., E. J. Merino, and K. M. Weeks.** 2006. Selective 2'-hydroxyl acylation analyzed by primer extension (SHAPE): quantitative RNA structure analysis at single nucleotide resolution. Nat Protoc **1:**1610-6.

Supplementary Figures

Supplementary Figure 1. eIF4G protein alignment. Identical residues are shaded grey and similar residues are white with black shading. Ascaris is *Ascaris suum* (ACX37244), Brugia is *Brugia malayi*

(XP_001895525, parasitic nematode), C. elegans is *Caenorhabditis elegans* (NP_001022259), bee is *Apis mellifera (*XP_393239), human is *Homo sapiens* eIF4GI (Q04637), and wheat is *Triticum aestivum (*Q03387). Boxed and arrowed regions indicate domains in the human eIF4GI.

Supplemental Figure 2. 5' monophosphate RNAs decay faster than capped RNAs and levels of uncapped RNAs are not different between the WT SL and SL Mut-3. A). Decay of monophosphate mRNA compared with capped RNAs during Ascaris cell-free translation. GMP RNAs were primed with GMP and thus contain a 5'-monophosphate. RNAs were analyzed as described in Figure 1 C. **B).** Assay for presence of decapped, 5'-monophosphate RNAs during translation. RNAs were isolated at the illustrated time points and treated with Terminator enzyme. Terminator enzyme degrades only 5'-monophosphate RNAs (not 5' capped, triphosphate, or diphosphate RNAs)(Epicentre, Madison, WI). The plots illustrate the amount of remaining RNA during translation that is resistant to terminator enzyme (e.g., capped RNA). Note that WT SL and the Mut-3 SL RNAs do not show significant differences in the degree of uncapped RNAs.

Supplemental Figure 3. Spliced leader sequences required for efficient translation. A). Multiple nucleotides within block 1 of the SL contribute to translation of TMG-capped RNAs. **B).** Multiple nucleotides within block 3 of the SL contribute to translation of TMG-capped RNAs. **Raw data for spacing analysis normalized in Figure 3. C).** Insertion mutations were designed with compensating deletions after the SL (e.g., SL-G+2N and -2N) to account for changes in the length of the 5' UTR on translation. The actual decrease in translation from the insertions (SL-G+XN) is greater when deletion mutations (-XN) are considered. These data were used to present normalized values in Figure 6 by dividing the translation level of the "SL-G+XN" value by the "-XN" value

Supplementary Figure 4. Mutations in block 3 of the spliced leader results in increased flexibility in both blocks 1 and 3 suggesting residues within these blocks interact. A). TMG-capped 64 nucleotide WT SL and GGGU MUT 3 RNAs were analyzed using SHAPE (3, 4). Mutations in nucleotides 10 – 13 (Block 3) caused increased flexibility in those nucleotides as well as near the cap, nucleotides 2 – 4 (Block 1). Marked in red are the nucleotides in blocks 1 and 3. **B).** Quantitation of

accessibility changes illustrated in A. Gels illustrated in A were subjected to phosphoimager analysis. Experiments were carried out as described in the Materials and Methods.

Supplementary Figure 5. m^7GTP-sepharose treatment of Ascaris extracts reduces eIF4G and eIF4E. Ascaris translation extract was treated with m^7GTP-sepharose and the amount of various proteins removed from the extract determined by Western Blotting. Antibodies to the Ascaris proteins were generated to full-length eIf4E-3, a truncated form of eIF4G, and peptides derived from the N-terminus of Ascaris eIF4E-1 and eIF4E-4 (Davis et al, unpublished).

Supplementary Figure 6. SL affects translation at the initiation step. A). Translation time course for WT SL and GGGT Mut-3 RNA. **B).** Translation time course for WT SL and GGGT Mut-3 RNA illustrating the linear phase of translation. **C).** Sucrose gradients of Ascaris Extract with WT SL and GGGT Mut-3 RNA. Experiments were carried out as described in the Materials and Methods.

Supplementary Figure 7. The SL stem loop does not increase Ascaris eIF4E/4G's affinity for TMG-capped RNAs. A). Ascaris eIF4E/G complex has the same affinity for the TMG-capped wild-type SL, stem-loop mutant, and compensatory stem-loop mutant. The figures illustrate the surface plasmon resonanse responses and residuals obtained for binding of varying concentrations of eIF4E/G to different immobilized RNAs. The burnt orange lines show best fit used for analysis. These data were used to calculate values shown in Table 1. Concentrations of eFI4E/G used were 1.73 nM, 3.45 nM, 6.9 nM, 13.8 nM, 27.6 nM. **B).** Translation inhibition assay using trimethylguanosine cap analog. Note that the cap analog does not differentially affect translation of the mRNAs. **C).** Ultraviolet light crosslinking of recombinant Ascaris eIF4E-3 to universally labeled RNAs. Experiments were performed as previously described (2).

Supplementary Figure 8. The C. elegans SL2 and hybrid SLs between SL1 and C. elegans SL2 variants support translation of a TMG-capped RNA. A). Analysis of translation of C. elegans SL2, hybrid spliced leaders, and other SL variants. **B).** Translation of Trichinella spliced leaders. Experiments were carried out as described in Figure 1. Blue sequences represent SL1 nucleotides, orange SL2 nucleotides, and green and purple nucleotides are variant in alternate SL2-like leaders

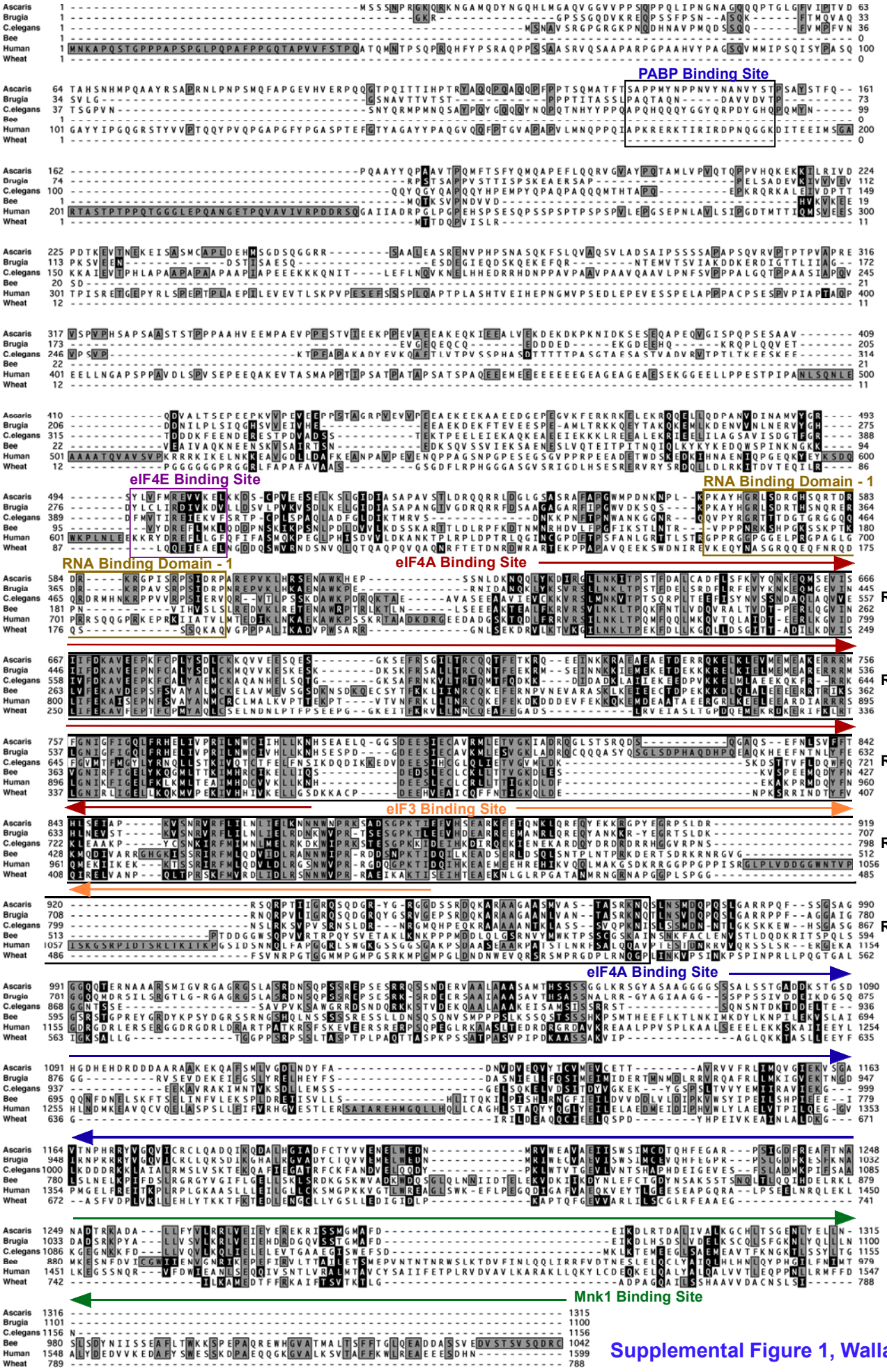

Supplemental Figure 1, Wallace et al.

A

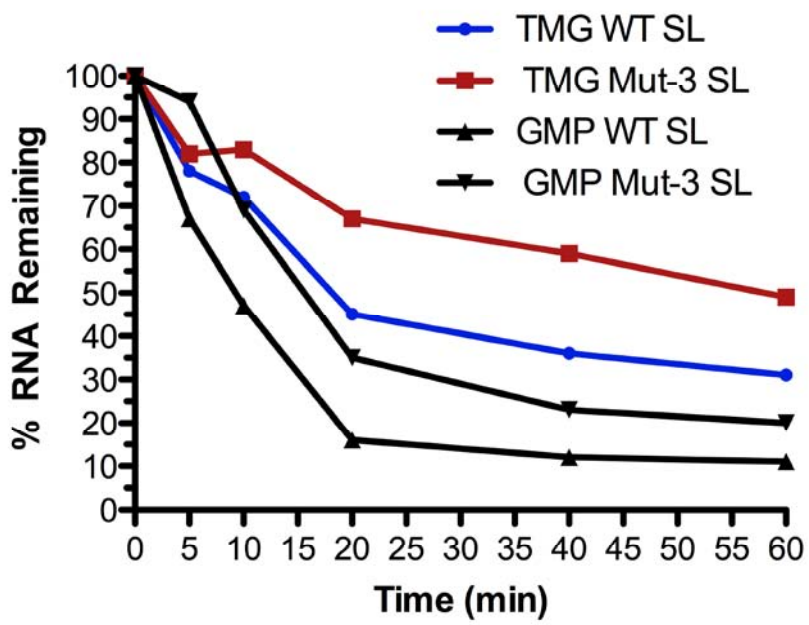

B

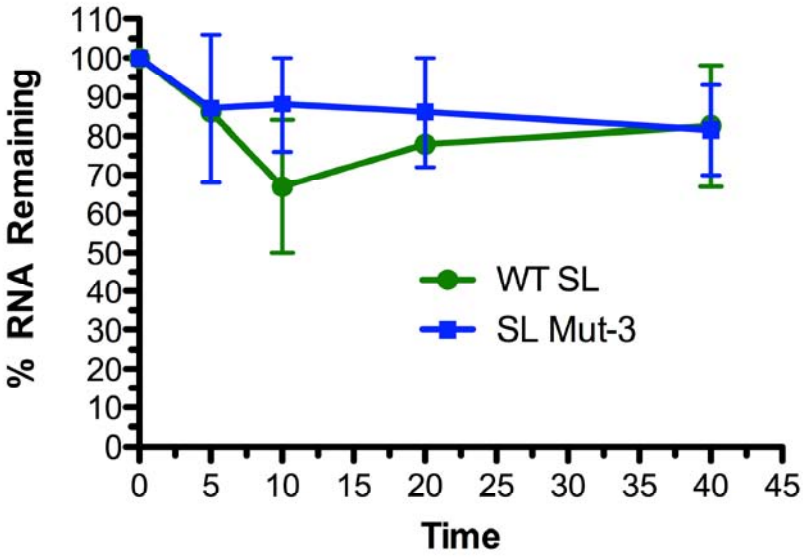

Supplemental Figure 2, Wallace et al.

Supplemental Figure 3, Wallace et al.

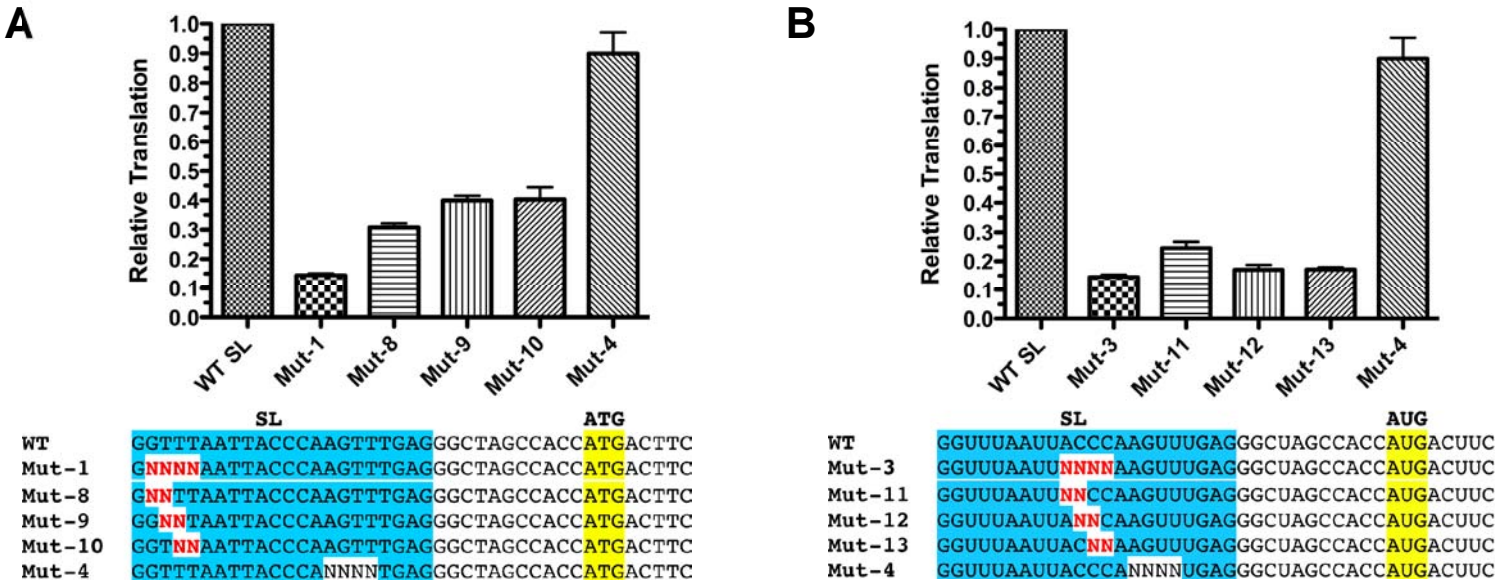

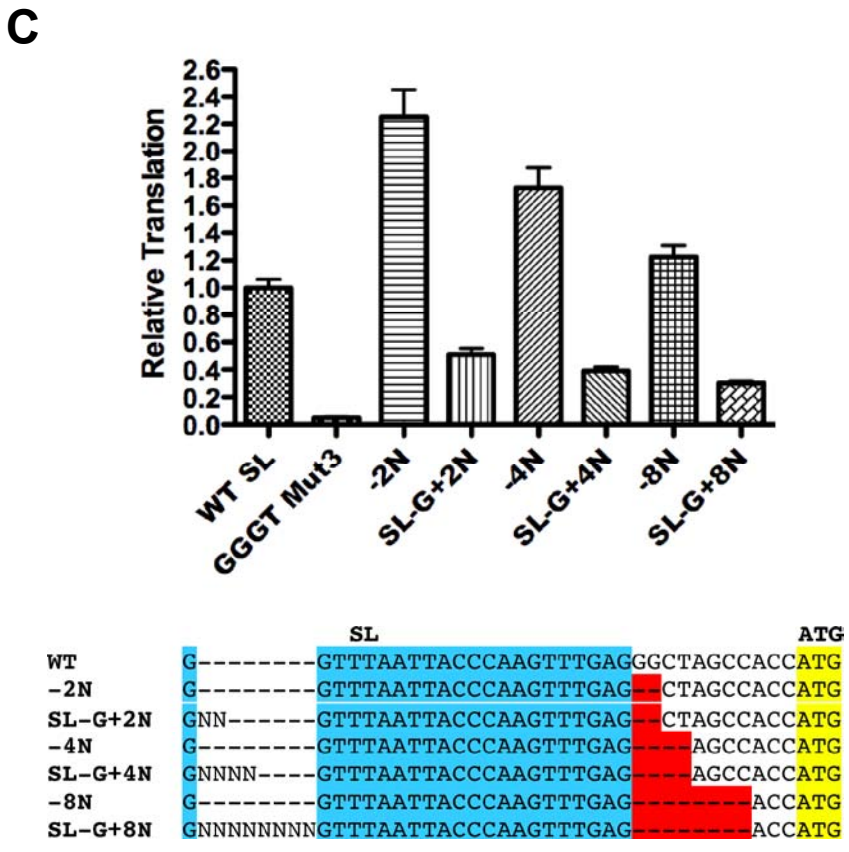

A

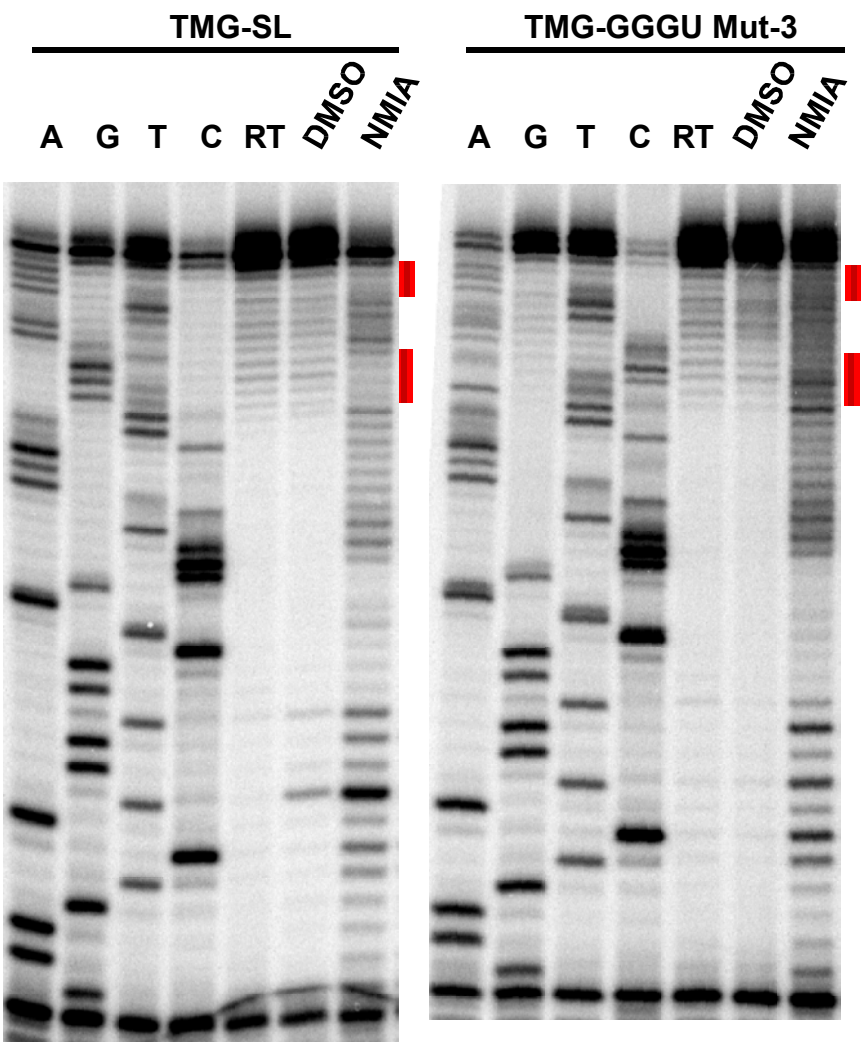

1 2 3 4 5 6 7 8 9 10 11 12 13 14 15 16 17 18 19 20 21 22

TMG-SL: TMGpppG-G-U-U-U-A-A-U-U-A-C-C-C-A-A-G-U-U-U-G-A-G

TMG-GGGU Mut3: TMGpppG-G-U-U-U-A-A-U-U-G-G-G-U-A-A-G-U-U-U-G-A-G

B

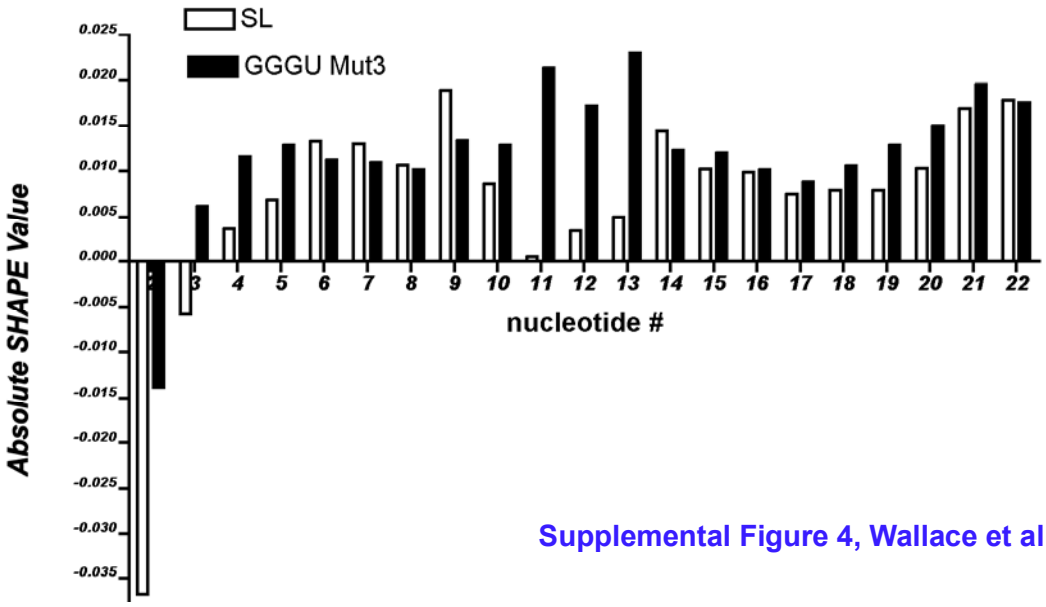

Supplemental Figure 4, Wallace et al.

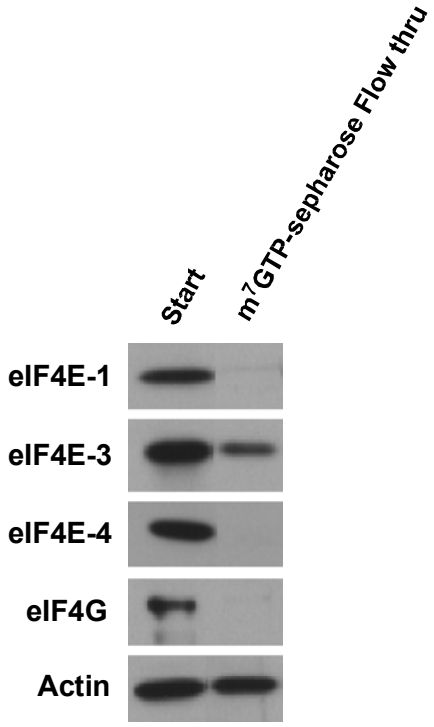

Supplemental Figure 5, Wallace et al.

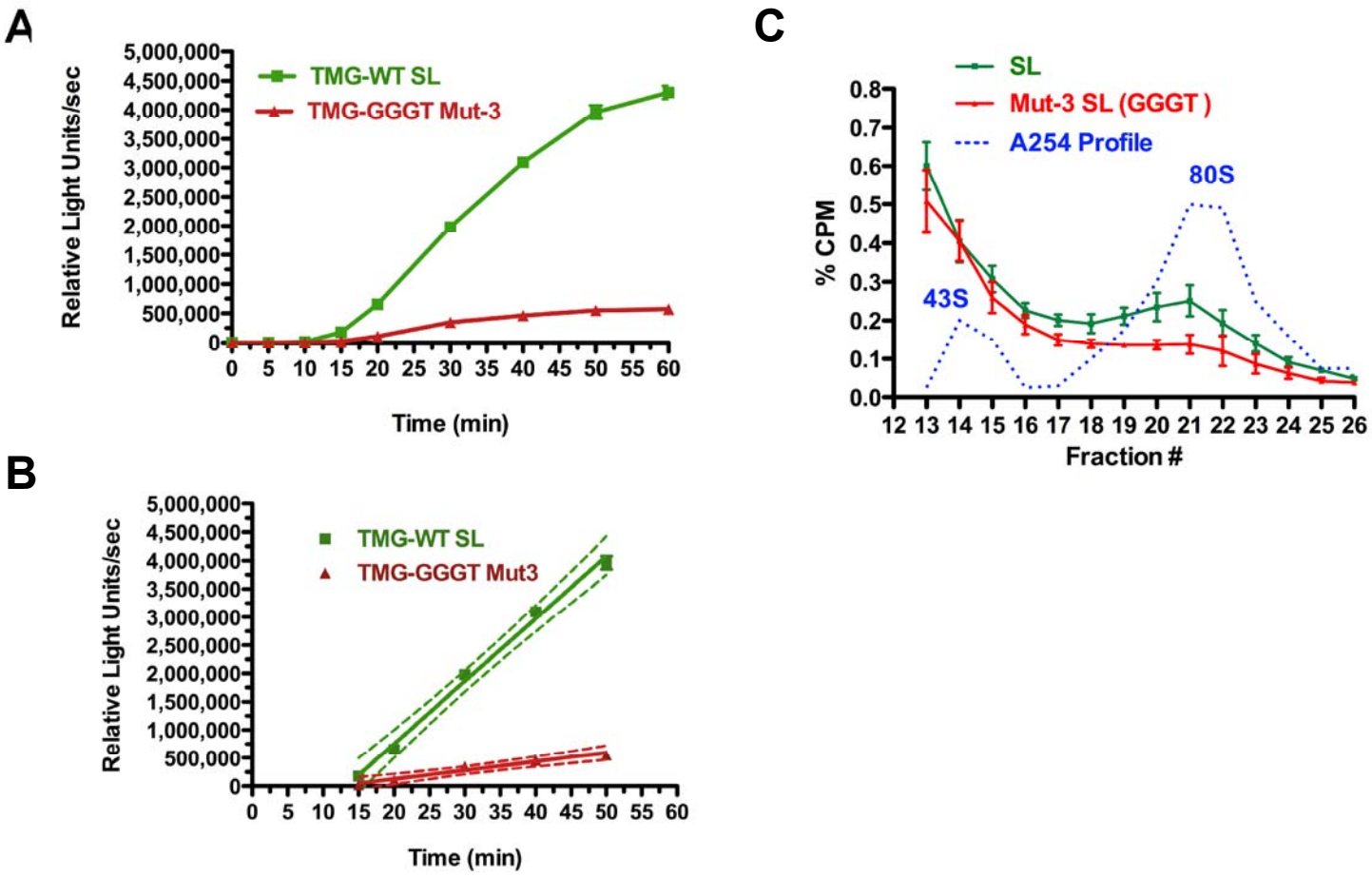

Supplemental Figure 6, Wallace et al.

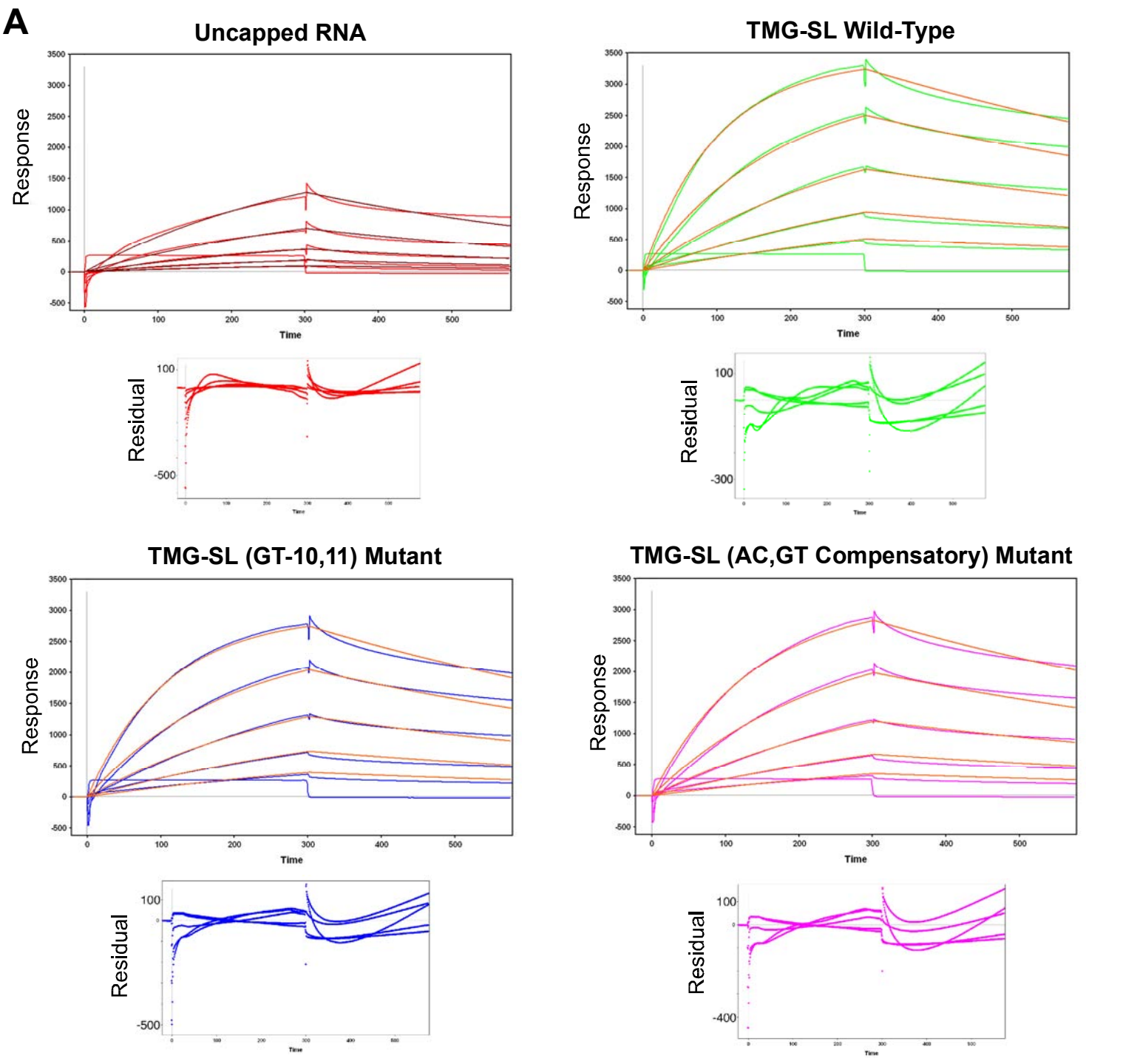

Supplemental Figure 7, Wallace et al.

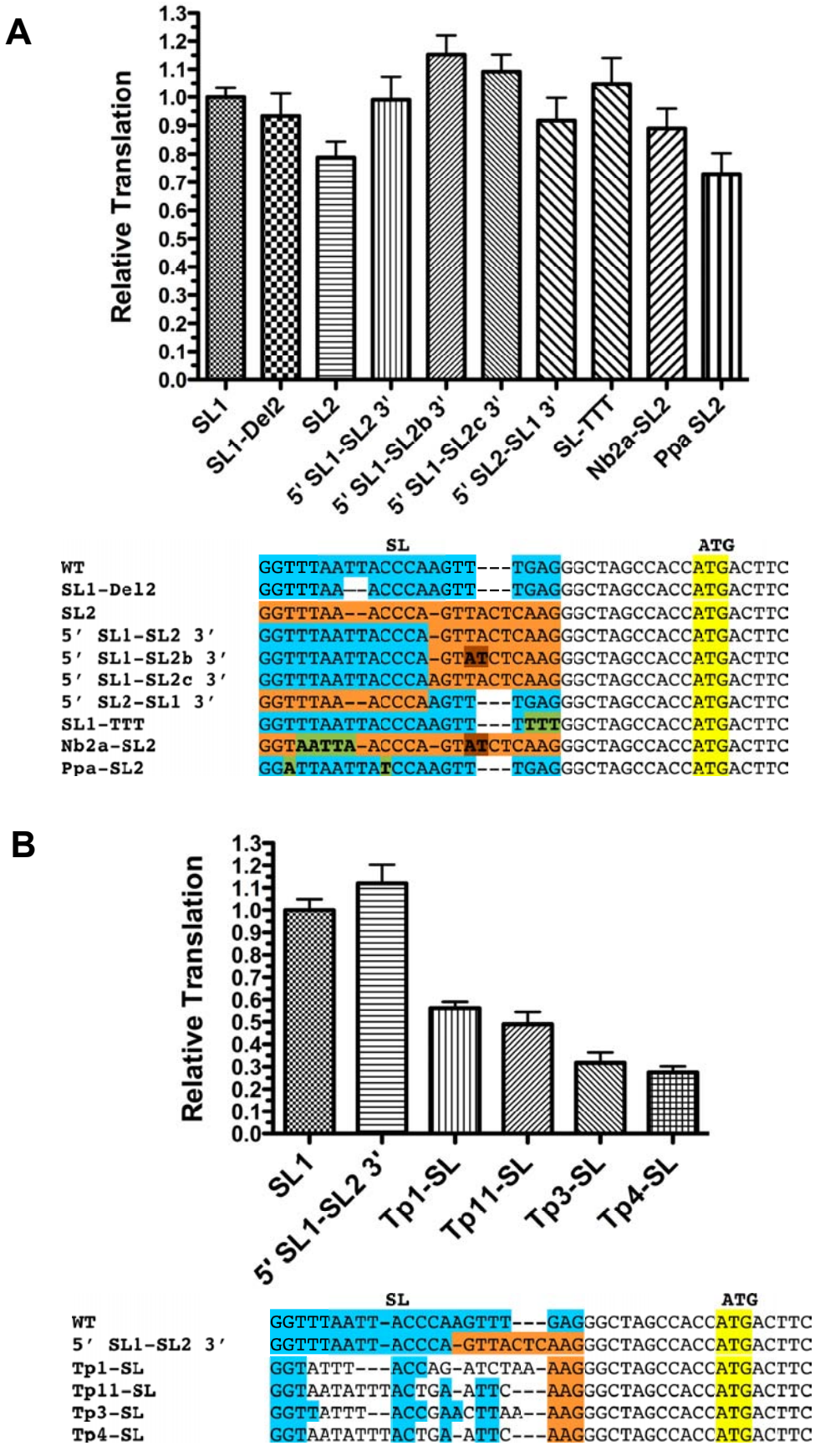

Supplemental Figure 8, Wallace et al.